NTNU – Trondheim
Norwegian University of
Science and Technology

Operation of IGBT-Modules in Insulation Liquids

A First Step for Enabling Operation in High Pressure Environments

Kristian Eikeland Holmefjord

Master of Energy and Environmental Engineering
Submission date: June 2015
Supervisor: Lars Einar Norum, ELKRAFT
Co-supervisor: Magnar Hernes, SINTEF Energy Research

Norwegian University of Science and Technology
Department of Electric Power Engineering

Problem Description

For subsea processing plants in oil and gas production, power converters can be used to increase the extraction amount from a reservoir. A 1 % increased total production on the Norwegian Continental Shelf is valued at 40 billion Euros [1].

SINTEF Energy Research, in cooperation with NTNU, has an ongoing project sponsored by The Research Council of Norway and industry partners. The objective is to provide fundamental material and packaging knowledge for the realization of reliable pressure tolerant power electronic components and circuits for operation depths down to 5000 m, corresponding to 500 bar. The idea is to place the converter in a vessel filled with a dielectric liquid. The vessel can then be pressure compensated to the external sea water pressure [2].

Submerging components in dielectric liquid under high pressure represents new environmental conditions for the power and control electronics. Assuming target pressure of 500 bar and components for medium voltage source converters (6.6 kV), this master thesis will give a review of following topics:

1. Provide basic component theory for converters.
2. Propose tests and qualification methods to verify operability of power electronic components in dielectric liquids.
3. Design and construct a high voltage test cell for live testing of components submerged in liquid.
4. Perform high voltage tests on power electronic components submerged in liquid and evaluate results.
5. Describe problems and modification to the high voltage test cell to provide guidance for future test setups.

Sources for information could be open published information, information from manufacturers and open information from SINTEF/NTNU projects.

Abstract

Theory regarding the main components needed in a subsea converter are provided. Focus is spent on the IGBT and pulse testing are described. A safe and fully functional test cell for high voltage single and double pulse tests was constructed and approved for operation by both NTNU and SINTEF Energy Research. A custom wounded air-inductance was constructed at the NTNU-workshop to act as a load for the pulse tests. The insulating liquids MIDEL and Galden are described. Humidity-requirements for the liquids are compared to IEC-standards and chosen at 5 % relative humidity in MIDEL and 25 % in Galden.

Characterization of components and successful high voltage pulse tests was performed. Tests were performed before, during and after liquid exposure. Two IGBTs was tested for a 14 day period, one in MIDEL and one in Galden. Both liquids gave sufficient electrical performance. Galden is regarded as the best filling liquid due to earlier research at SINTEF Energy Research where some material compatibility-issues with MIDEL was found.

Modification while constructing the test-cell and during tests are described. Optical communication in MIDEL gave a weakening of the fibre optical-link. In realizing a full size converter with optical communication, it is important to account for these losses when dimensioning the strength of the sender.

Sammendrag

Teori om hovedkomponentene i en trykkbasert kraftelektronikk-konverter er presentert. Fokuset er på IGBT-en og hvilke testmetodikker som kan brukes for å redegjøre for funksjonalitet av en IGBT i væsker. Deriblant er enkel- og dobbelpuls testing av IGBT-er forklart. En høyspent test-celle for pulstesting er designet og konstruert. Cellen er blitt sikkerhetsklarert av både NTNU og Sintef Energi for spenning opp til 6.5 kV. For å gjennomføre pulstester ble en spesialviklet luft-spole laget på NTNU-verkstedet som skal være last på testene. Fuktighetskrav til testvæskene er satt i henhold til IEC-standard for luftfuktighet. 5 % relativ fuktighet ble brukt i MIDEL og 25 % i Galden.

Karakterisering av test-komponentene ble gjennomført før og etter de ble utsatt for isolasjonsvæskene. To IGBT-er ble testet i 14 dager, en i MIDEL og en i Galden. Resultat fra testene viste at begge væskene var elektrisk kompatible til å brukes i en trykktolerant konverter. MIDEL har fra tidligere forsøk hos SINTEF Energi vist at den har et kompatibilitetsproblem med gel-en som ligger på IGBT-er. Galden er derfor anbefalt som den isolasjonsvæsken det bør gjennomføres videre trykksatte langtidstester på.

Modifikasjoner og sikkerhetsfunksjoner for høyspentcellen er forklart. Et viktig resultat fra væsketestene er at optisk kommunikasjon gjennom fiber blir svekket av å være omgitt av væske. Dette er noe man må ta høyde for når man designer en konverter ved å dimensjonere kraftigere sendere.

Preface

This master thesis is the final work for my Master of Science at the department of Electric Power Engineering at the Norwegian University of Science and Technology.

The beginning of this work explains why there is a need for subsea converters. The main components in a converter is mentioned, and theory regarding these components are explained. Definitions and characterizations of the test components are performed. The complete test setup and plans for testing of the equipment are described. Results of the planed tests are presented.

There has been a large focus on safety during this project, as a high voltage test-cell has been constructed inside an empty cabinet. Kjell Ljøkelsøy and Ole Christian Spro at SINTEF Energy Research has been of great help to ensure safe operation of the test cell.

Thanks to my supervisors Senior Research Scientist Magnar Hernes at SINTEF Energy Research and Professor Lars Norum at NTNU, for their guidance during this project.

Kristian Eikeland Holmefjord

Trondheim, June 2015

Table of Content

List of Figures

List of Tables

Abbreviations

BJT	-	Bipolar Junction Transistor
DC	-	Direct Current
FPGA	-	Field-Programmable Gate Array
FWD	-	Free Wheeling Diode
IEC	-	International Electrotechnical Commission
IGBT	-	Insulated Gate Bipolar Transistor
LFS	-	"Leder for Sikkerhet" (Chief of Security)
MOSFET	-	Metal-Oxide Semiconductor Field Effect Transistor
NTNU	-	Norwegian University of Technology and Science
RH	-	Relative Humidity
SiO_2	-	Silicon Dioxide
VAC	-	Voltage Alternating Current
VSC	-	Voltage Source Converter

1 Introduction

There is currently a large increase in planned subsea oil and gas installations, with high power demands. Transmission and control of subsea equipment is a challenge, where utilities on the seabed have different power requirements. The present way of resolving this problem is to have power electronics on an offshore platform or onshore, and transmitting power to each utility separately. There are several challenges associated with installing power electronics on offshore platforms. The mixture of humid air, seawater and power electronics requires the converter stations to be built into closed modules. The modules will then consume valuable space on the platform. One of the biggest disadvantages with utilizing topside converter stations is the complex cable and riser systems on the AC side, where each load requires a separate cable. The cable-length from converter to utilities on satellite-wells creates a problem in controllability and efficiency. In addition, there may be different demands on voltage and frequency for different loads [3]. On a field in the Gulf of Mexico, they approximate an increased total production of 20-30 % by installing topside compressors. Subsea compressors could have an even higher production increase, depending on the field. A 1 % increase in total production on the whole Norwegian Continental Shelf is valued at 40 billion Euros [1].

The future subsea converter design is predicted to be a completely pressure compensated solution, which is the focus of this report. Several large companies are already working on this solution and SINTEF Energy Research has a research project focused on this concept. If a converter can be designed in a pressure compensated vessel, it means that there will be no forces acting on the module wall, which could reduce the wall thickness by up to 90 % [2]. Easier installation and cooling of power electronics through natural convection is among the benefits. This gives the possibility of creating a cheaper and more reliable converter.

There are several uncertain factors of designing this solution. This report focus on the power electronic issues arising in this design. Special attention is put on how considered filling liquids influences the IGBT and other components inside the subsea converter.

2 Theory

The theoretical part is mainly regarding the IGBT. This is a crucial component in realizing a subsea converter solution. Earlier studies at SINTEF Energy Research has proven constant electrical properties on IGBTs when exposed to a pressurized environment [4]. This is why all tests will be performed at atmospheric pressure.

2.1 Insulated Gate Bipolar Transistor (IGBT)

The generic operation and structural design of the IGBT is thoroughly described in other literature [5-7], as well as in the specialization project leading up to this work [3]. A basic explanation of the IGBT is included here while the focus will be on theory regarding an IGBT-module in liquid, and how to test the unit in liquid.

Insulated Gate Bipolar Transistor is a semiconductor switch, which combines the controllability of a MOSFET and the conducting properties of a bipolar transistor. In recent years, advances of the IGBT has led to it being the most applicable and efficient semiconductor for medium voltage drives. The continuous development for reduced losses and high power ratings is one of the reasons why the IGBT is assumed to be the dominant semiconductor-switch in subsea power systems.

This thesis will only focus on planar IGBT modules, as this is the semiconductor switch that will be tested experimentally in liquid. The bonded planar IGBT is the most popular IGBT-design in the market today. SINTEF Energy Research has earlier successfully tested a customized pressurized press-pack IGBT [8]. Press-pack IGBTs are therefore not tested in this thesis. Complementary information regarding pressurized press-pack solutions can be found in SINTEF Energy Research publications and the specialization project leading up to this work [2, 3, 8, 9]. Figure 1 illustrates an IGBT module filled with gel. The insulating liquid will thus only be in contact with the gel, shielding the areas of high electric fields from impurities in the liquid. The IGBT module used in the liquid tests are further described in chapter 5.1.

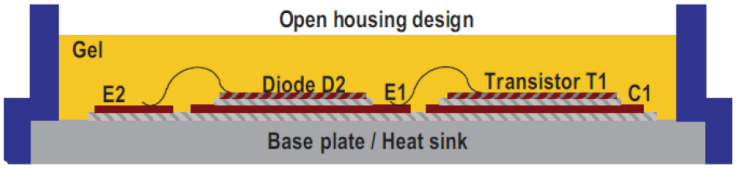

Figure 1 - IGBT module with gel (Yellow) [10]

2.1.1 Guard Rings

One of the reasons for a breakdown in an IGBT is caused by high electric fields. In the structural design of the IGBT, guard rings are introduced to control the electric field on the surface of the chips. The guard rings have a floating electrical potential, and will prevent breakdown at full reverse bias voltage even though the distance/curvature are small [5]. An illustration of how the guard rings are implemented in a pn-junction diode is shown in figure 2. The guard rings in this figure will prevent the depletion layer from having too small a radius of curvature.

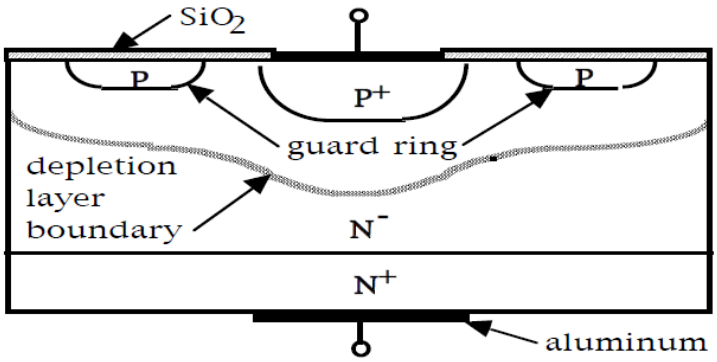

Figure 2 - A PN-junction diode with guard rings [5]

Silicon dioxide (SiO_2) is used as extra coating to aid in controlling the electric field at the surface. A standard IGBT module is usually delivered with this type of protective gel. For the SINTEF Energy Research project, a few IGBTs has been delivered without the silicone gel. This will allow for testing only with insulating liquid, or with a self-applied gel. An illustration of one proposed solution without gel is shown in figure 3, where it is used a thin coating for chip protection. This solution puts extremely high demands for purity in the insulating liquid. The manufacturers of IBGTs will not reveal what coating-solution they use in the trenches on the IGBT substrate or between the chip and the gel. One of the trenches on the IGBT is shown in the red circle in figure 3. As the high electric field is not extra protected by gel, any impurities will be dragged towards this area, which could lead to a breakdown of the IGBT. The coating could be a nitride or polyimide-layer. This proposed protection method will increase cooling-efficiency since the insulating liquid will be very close to the heated chips on the IGBT during continuous operation.

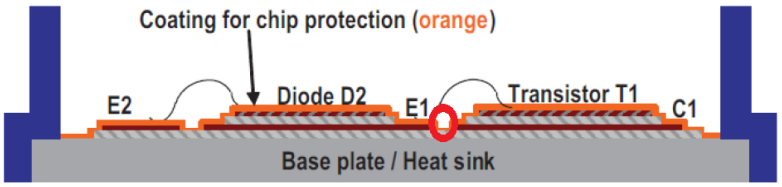

Figure 3 - IGBT module without gel [8]

2.1.2 Switching Waveforms of IGBTs

The switching of an IGBT are associated with high peak power dissipation pulses, due to the combination of a high DC-link voltage and large output current. It is important that the values of voltage and current are kept within the Reverse Biased Safe Operating Area. To operate the IGBT outside this area can be destructive for the device [8]. The turn-on current and voltage for an IGBT in a step up/down converter is shown in figure 4. In pulse testing, a similar turn-on curve will be seen. However, the output current I_O will be linearly increasing in the test-setup due to the load inductance. The timeframe can vary between IGBTs, but a typical turn-on can take approximately 0.33 µs [11].

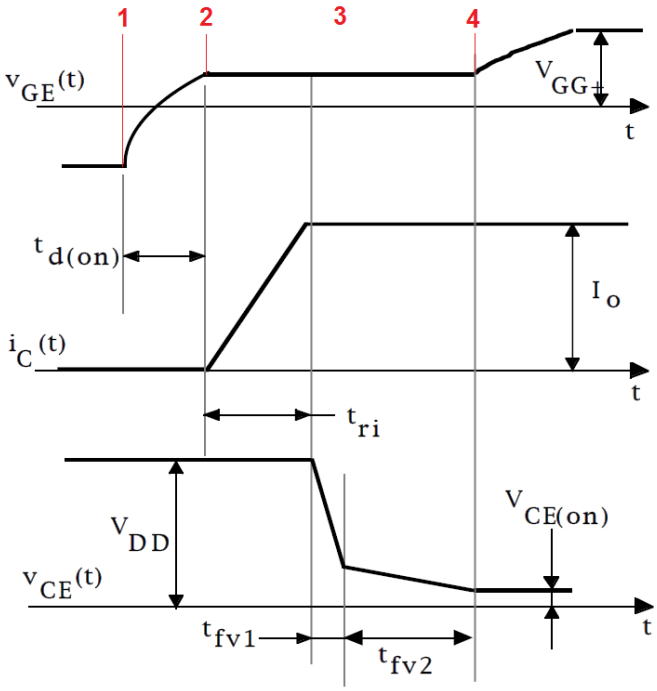

Figure 4 - Turn-on waveforms [5]

A thorough explanation of each part, including doping-levels and conductivity modulation of the IGBT is explained in literature [5, 6, 12]. A step-by-step explanation of the turn-on referring to figure 4 can be summarized as following:

1. The gate driver applies a step voltage to the gate-emitter terminals, leading to a charge of the input capacitance on the IGBT.
2. At $V_{GE}=V_{GE(Threshold)}$, where threshold is given in the datasheet, $I_{collector}$ will start to increase linearly. There is a trade-off between having a fast T_{fv2} and a low $V_{CE(on)}$.
3. V_{GE}=Constant until $V_{CE}=V_{CE(on)}$, where $V_{CE(on)}$ is the forward voltage drop explained and measured in chapter 5.1.3.
4. V_{GE} increases to output voltage from the gate driver and the IGBT is fully turned on.

A similar transient can be found at turn-off of the IGBT seen in figure 5. A turn-off is often somewhat longer, due a larger gate turn-off resistance, giving a typical turn-off time of 0.40 µs [11]. A step-by-step explanation referring to figure 5 is summarized below.

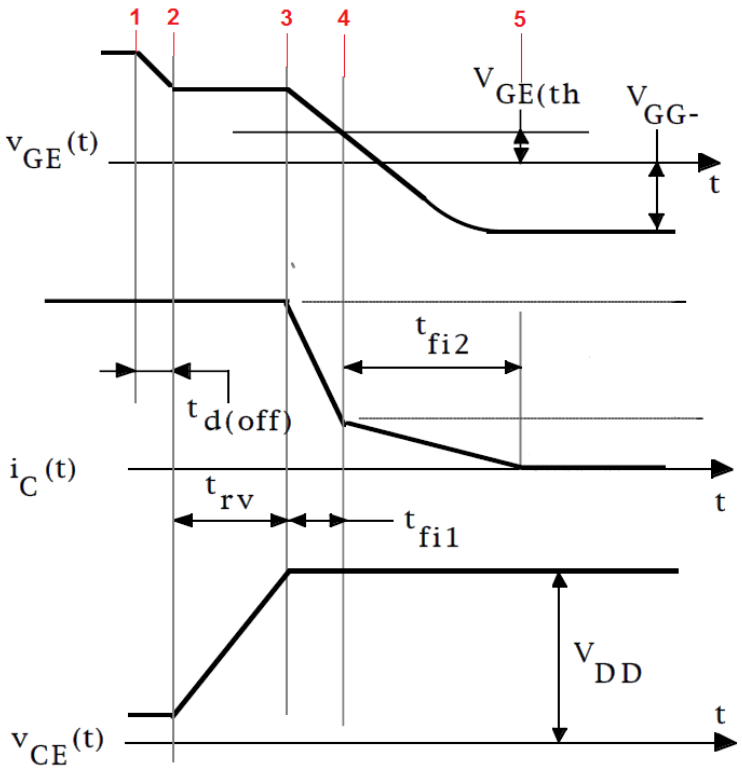

Figure 5 - Turn-off waveforms [5]

1. The gate driver applies a negative gate-emitter voltage, resulting in a discharge of the input capacitance on the IGBT.
2. The voltage starts to increase linearly across the IGBT while V_{GE} is kept constant.
3. V_{CE} has reached DC-link voltage and I_C starts to decrease, leading the current through the freewheeling diode. The decrease is controlled by two different mechanisms, the MOSFET mechanism causes a rapid decrease, and the BJT mechanism causes a slow decrease. Further explanation of this can be found in [3, 5, 6].
4. V_{GE} reaches $V_{GE(Threshold)}$, the MOSFET portion of the current-decrease is done and the less steep BJT portion continues to reduce the collector current.
5. The IGBT is fully turned off and V_{GE} stabilizes on the gate driver turn-off voltage.

Switching of IGBTs generates a high amount of losses. A fast switch reduces a single switch-loss while a high switching frequency will increase the total losses. An efficient cooling solution is needed to transport the heat from switching and forward voltage losses. In IEC 60747-9, specifications for calculating the switching energy dissipation using the double pulse test method can be found [13]. An illustration of the energy calculations at turn-on and turn-off are shown in figure 6.

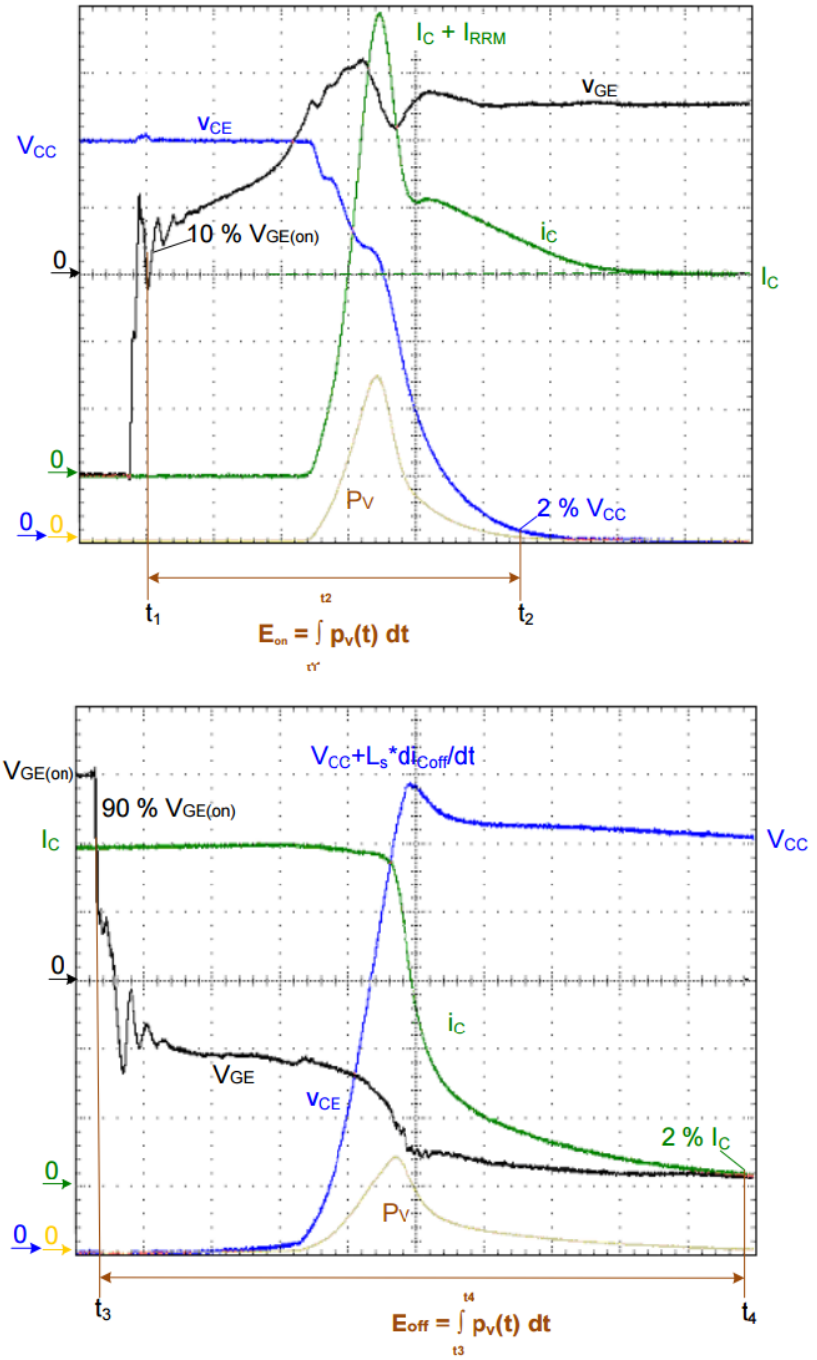

Figure 6 - Switching losses according to IEC 60747-9 [13]

2.1.3 Single and Double Pulse Testing of IGBTs

Pulse testing of IGBTs are an efficient way of testing the behaviour and characteristics of IGBTs using only a small amount of power. The double pulse test is the preferred test to perform, as it can be used to test a large variety of conditions. These can be summarized as following [6]:

- Behaviour at different temperature and humidity levels.
- Measuring of switching losses.
- Diode recovery current.
- Short-circuit behaviour and short-circuit shutdown
- Behaviour of the gate drive, which can involve adjustment of R_{Gon} and R_{Goff}.
- Overvoltage behaviour at turn-off, which involves adjustment of active clamping.
- Current distribution over modules when connected in parallel.

The single pulse test will be used to see if any breakdown happens. In a single pulse test, the pulse can be longer than the double pulse, since the collector current can go to its maximum value during one on-period. A setup for single and double pulse testing is shown in figure 7.

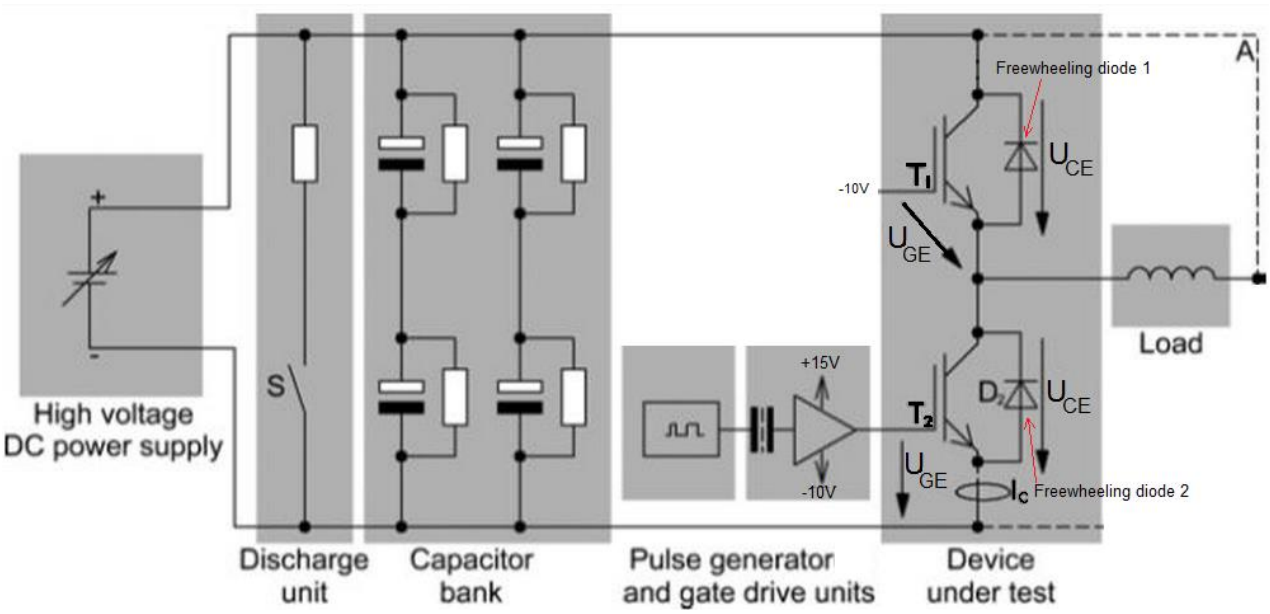

Figure 7 - Test setup for pulse testing of lower IGBT and upper diode [13]

The pulse-generator was replaced with an FPGA-board and interface boards to increase the controllability in the test-setup of this thesis. The DC-bus is designed using thin and flexible bus bar which reduces inductance and therefore limits transient overvoltage when switching.

An example of a double pulse test is shown in figure 8. The values t_1, t_2 and t_3 are adjusted so that the maximum current at the second turn-off is approximately nominal IGBT current. T_4 is defined as the time between each time this double pulse scenario is performed, and must be high enough to keep the DC-link stabile. A high t_4 (1-5 seconds) also ensures that there is no temperature-increase due to switching losses which means that the tests can be performed in stable surroundings.

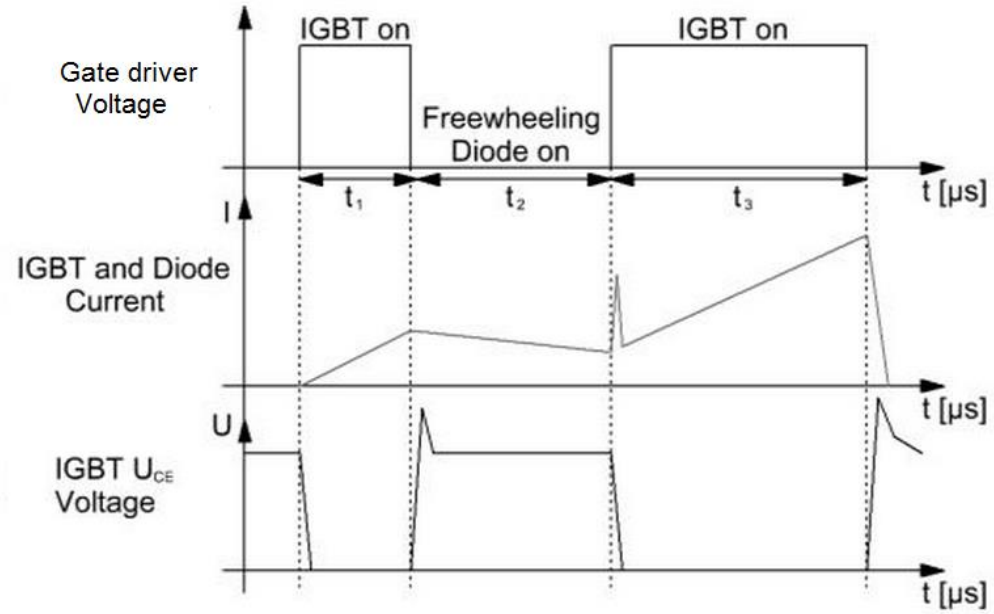

Figure 8 - Double pulse test [13]

At the first turn-on pulse, a current is established through the load inductance. The first turn-off creates a current in the free-wheeling diode. The high inductance and low resistance of the load gives a very low decrease in the current during the off-period t_2. At the second turn-on pulse there is a reverse recovery in the diode, which leads to a current overshoot similar to a real life application. At the second turn-off, the overvoltage is the highest. This value must be kept below the IGBTs blocking voltage V_{ces} by minimizing the stray inductance. The use of an adjustable load inductance and variations in pulse lengths gives the opportunity to simulate different load conditions for the IGBT [14].

The change in inductor current will be defined by the voltage across the inductor and the inductance itself given by the formula:

$$\frac{di_L}{dt} = \frac{V_L}{L} \qquad \text{(Eq. 2.1)}$$

2.2 Capacitor

The high voltage DC source pre-charges the capacitor to ensure that there is enough power stored at the time when the pulse test is switched on. In converter-operation, the capacitor-bank keeps the DC-link at a constant value. The capacitors must have a large power capacity, as well as a high voltage rating. The advantages and disadvantages of different capacitors type are well described in the specialization project thesis up to this work [3]. The preferable and most used capacitor is the metalized film capacitor. A film capacitor is therefore tested together with the IGBT in the different liquids. The capacitor properties are further described in chapter 5.2.

SINTEF Energy Research are currently running a test on how a metalized film capacitor reacts to a pressurized environment. In pressure there have been some troubles regarding self-healing of the capacitor. The principle of self-healing is to avoid any permanent short-circuit in the dielectric material. In the event of short-circuit between the electrodes, a high current will melt the metalized electrode-area around the dielectric short in the film. An illustration of self-healing is shown in figure 9.

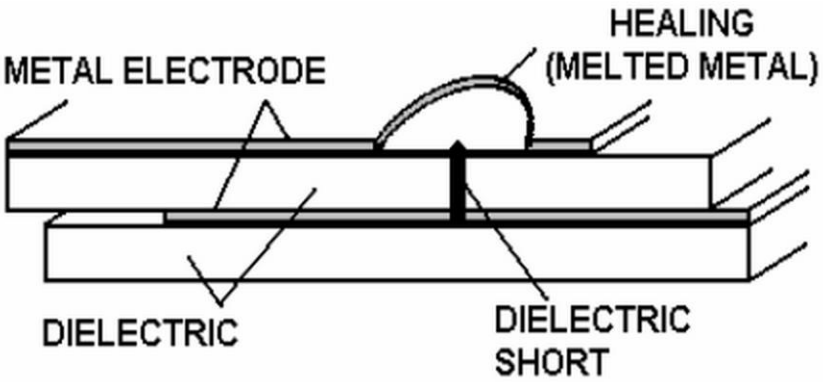

Figure 9 - Self-healing in a metalized film capacitor [15]

The film capacitor used in the tests in this thesis is assumed operable with the test-liquids since SINTEF Energy Research has had successful tests using a similar capacitor without pressure earlier. Measurements are performed before and after liquid-tests to ensure that the capacitor do not have any property degradations when to exposed to liquids.

2.3 Gate Driver

The gate driver circuit is the interface between the low voltage control signal and the high voltage switching at the IGBT. Its main function is to reproduces the low power control signal at a higher power level. The gate driver can also include protection mechanisms such as active clamping, which is used to reduce transient overvoltage at turn-off. The gate driver have to be located close to the IGBT and is therefore also tested in the insulating liquids, as it is a crucial component for reliable operations of a converter. A galvanic isolation between the IGBT and the control system is provided by the gate driver. The gate driver provides a reverse bias to the power circuit to ensure that no stray transient signals triggers the IGBT to switch in its off-period. It is also designed to minimize turn-on and turn-off times for loss-reduction. [5]. The layout of the gate driver circuit is important to optimize for minimum stray inductance. To avoid upper and lower IGBT in a bridge leg to turn on at the same time, a protection is often implemented on the gate drive. A simplified illustration of a gate driver, controlled by optical signals is shown in figure 10. The galvanic split DC-power supply are seen in the bottom left part of the picture.

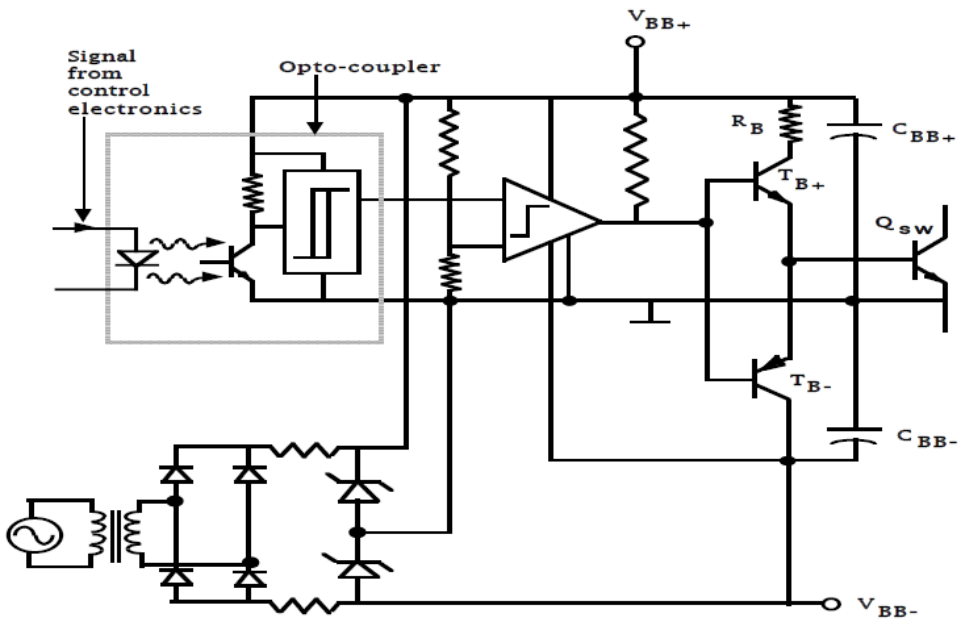

Figure 10 - Gate driver circuit [5]

3 Test-setup and Hardware

This chapter gives the detailed wiring and setup needed to perform tests described in chapter 2.1. No continuous current will flow in pulse-testing, thereby eliminating the need of cooling. The setup includes many other components than the actual IGBT, DC-link capacitor and gate driver. All different hardware and software used for the tests are described in this chapter. The IGBT, capacitor and gate driver are described in chapter 5.

3.1 Wiring Diagram

A complete one-line diagram for the test-setup is presented in figure 11. The colour of the measuring-points corresponds to the colour of the curves displayed on the oscilloscope in the results in chapter 7.

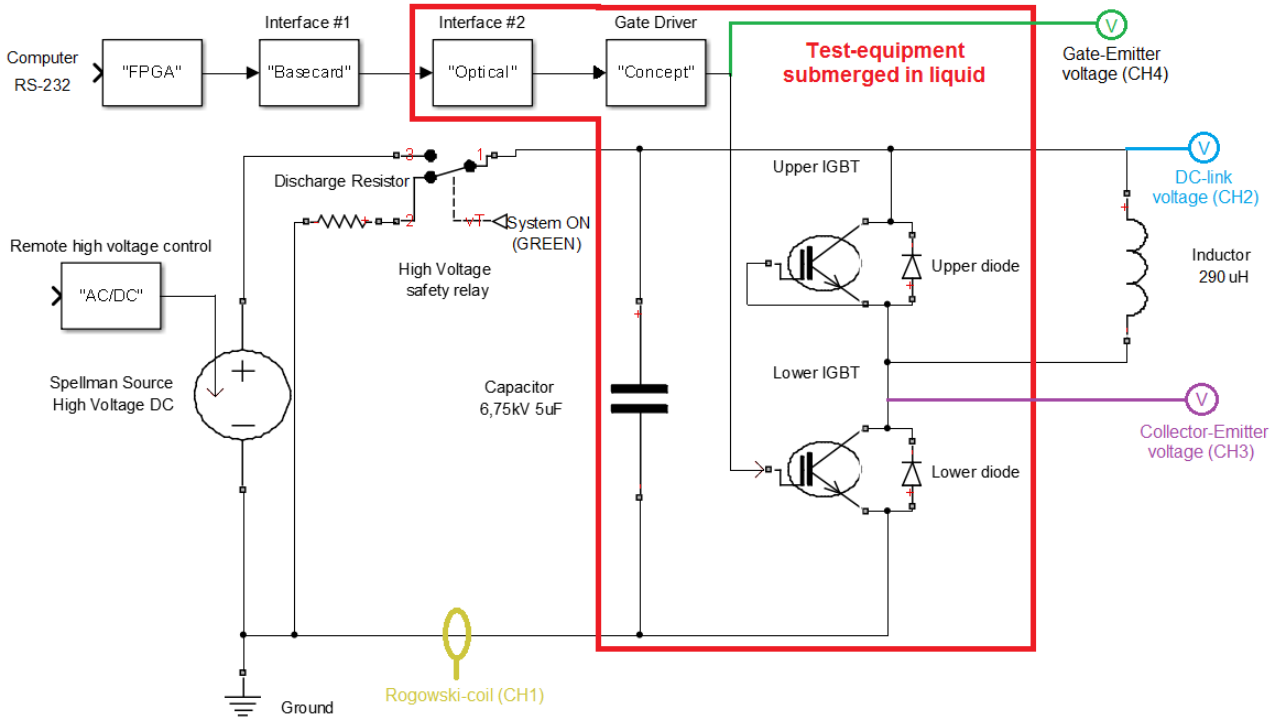

Figure 11 - Wiring diagram of test setup

3.2 Hardware

3.2.1 The Glass Container, Lid and Liquid-setup

To submerge the test-components in liquid, a glass-container was acquired. To protect the content from the surroundings, keeping a constant humidity and avoid contaminations of test-liquids, a custom cut lid was made. This was made in Polyoxymethylene by the NTNU workshop, together with brackets and an aluminium plate to attach test-components on. A rubber seal was put between the lid and the glass to ensure no contamination from the surroundings. The setup submerged in MIDEL is shown in figure 12. The lid serves as a rack for the test equipment with HV-bushings and a signal-penetrator mounted on top.

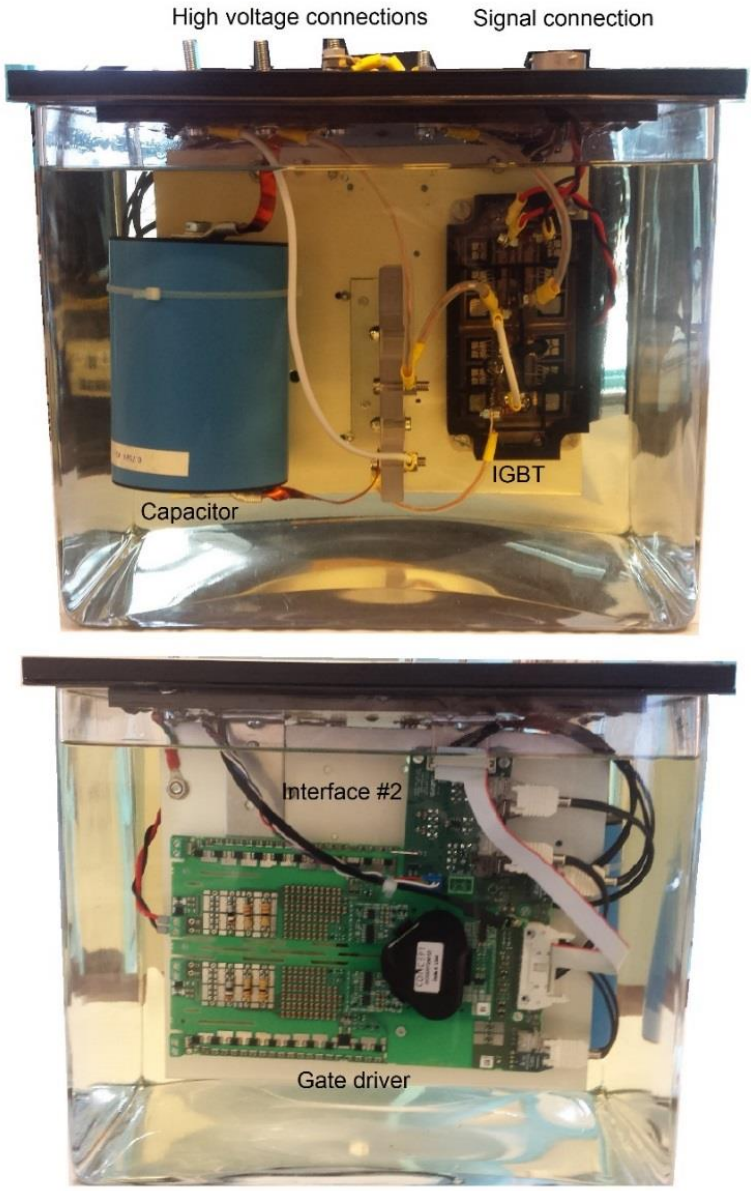

Figure 12 - Front and backside of test-setup submerged in MIDEL

3.2.2 Spellman SL30*300

The Spellman SL30*300 is a high impedance, high voltage source. It can deliver up to 10 mA at 30 kV. This source is used for charging the DC-link before a pulse-test. It is also used in the characterization of the IGBT for the voltage capability test and leakage current test. The voltage source is operated remotely by connecting a low voltage dc-source to the back-panel of the Spellman. Additional information is found in the instruction manual and datasheet [16].

Figure 13 - Spellman SL30*300 High voltage source

3.2.3 PL303-P Power Supply

The PL303-P is used for the remote control of the Spellman source. It is a linear correlation between 0-10 V on the PL303-P and 0-30 kV on the Spellman. A small voltage-change on the remote correlate to a large change on the Spellman-source. For safety, a 2.1 V Zener-diode was put on the output, parallel to the remote output to ensure that the Spellman-source never gave more than 6.5 kV. This power supply is used because it has an extra precise button marked "fine" on the voltage-settings, which ensure an accurate high voltage output.

3.2.4 High Voltage Safety Relay

A high voltage relay made at NTNU is used to disconnect and connect the capacitor to the high voltage source. The relay is driven by 230 VAC. Figure 11 shows how the relay is connected in the wiring diagram together with a resistor to ensure safe discharge off the capacitor.

3.2.5 Load-Inductance

A custom built circular air-inductance has been constructed at the NTNU workshop and is seen in figure 14. It was designed to have a high inductance, low resistance and still fit inside the test cabinet. A 2.24 mm^2 round wire was twisted around a 16 cm in diameter tube. It is twisted in two half-circles from the left connection-terminal to the right. This prevents a high voltage difference in any of the turns. An estimation of the inductance with a total of 103 turns in the coil using equation 3.1 gave a value of 267 µH. The length of wire needed to achieve this inductance gave an estimated DC-resistance of 0.11 Ω.

$$L = \frac{\mu * N^2 * A}{l} \qquad R = \rho * \frac{l_w}{A_w} \qquad (Eq\ 3.1)$$

where:

L = Load-inductance
μ = Permeability of air
N = Number of turns of the solenoid
A = Cross-sectional area of the solenoid
l = Length of the solenoid

R = DC-resistance
ρ = Resistivity of the wire
l_w = Length of wire
A_w = Cross-sectional area of wire

The wires were moulded with epoxy to fix their positions. When the coil was finished, a RLC-meter (Fluke PM306) was used to verify the performance of the inductor. The results are presented in table 1.

Table 1 - Characterization of inductance

Test frequency	Inductance	Resistance
50 Hz	294.0 μH	0.125 Ω
500 Hz	292.4 μH	0.126 Ω
5 000 Hz	291.7 μH	0.175 Ω
50 000 Hz	288.6 μH	0.546 Ω
500 000 Hz	284.0 μH	1.963 Ω

As seen in the table, the inductance was a bit higher than estimated. The estimation is based on a perfect round circle of each turn and a constant length between each wire. Most of the turns were somewhat bigger than 16 cm in diameter, which leads to a larger cross-sectional area, and therefore a larger inductance compared to the calculated value. The resistance is very close to the calculated values. Resistance increases at higher frequencies due to skin effect and proximity effect. The stray capacitance in the windings reduces the inductance at high frequencies.

Figure 14 - The custom wound load-inductance of 294μH

3.2.6 Control Rack

The control rack consist of three different components. The main component is a FPGA-board used to run the single and double pulse testing. The two others are a TRACO power supply and the interface card between the FPGA-board and optical interface board. All three components are shown in figure 15.

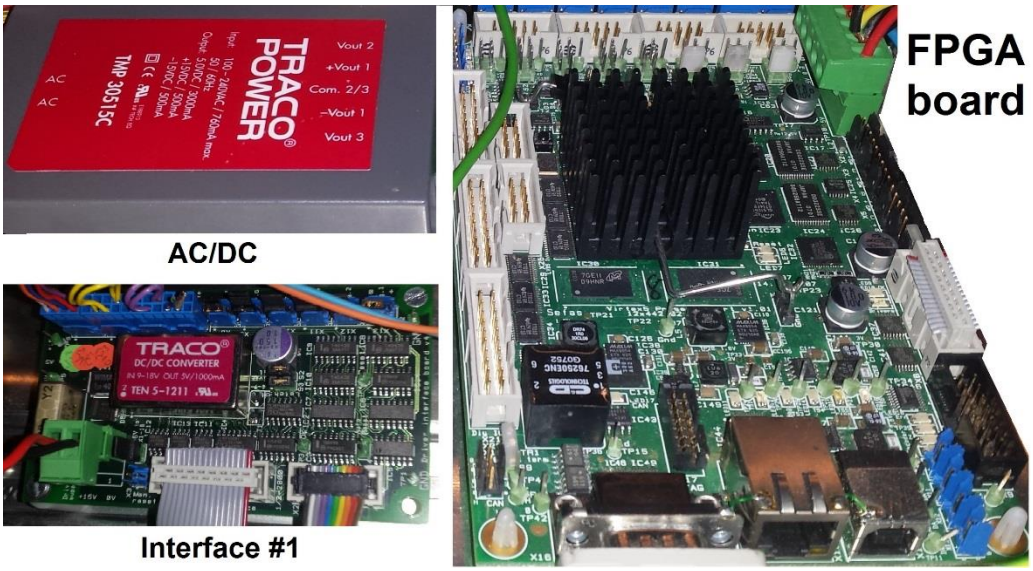

Figure 15 - Control cards mounted on control rack

3.2.7 Sensirion SHTxx EK-H4 V1.5

A Sensirion humidity and temperature sensor is used to monitor the relative humidity in the liquid, and observe that there is no temperature increase inside the test-container during tests. The sensor have earlier been successfully tested in MIDEL and is placed inside the glass-container together with the test-equipment.

3.2.8 Keithley 169 Multimeter

The Keithley 196 is a battery-driven multimeter used to measure the leakage current in the IGBT. The advantage of being battery-driven is that when measuring the current between earth and emitter, a high voltage potential is avoided in the measuring-devices. The measurement is described and illustrated in chapter 5.1.2 and in figure 24. This multimeter is set to measure in the 0-200 µA range.

3.2.9 Rogowski Coil

A Rogowski coil (PEM CWT 3R 600A) is used to measure the emitter current through the lower IGBT when it is turned on. The coil is placed on the top of the test-plate where the emitter-current is transmitted in a very small loop. Reasons for using a Rogowski-coil instead of a LEM-shunt or current-probe are further discussed in chapter 6.1.

3.2.10 Oscilloscope Tektronix MSO 2024B

A Tektronix Oscilloscope was used to perform the measurements shown in the chapter 7. Channel connections to the oscilloscope are as follows: the Rogowski current-coil (CH1), two high voltage probes (CH2 and CH3) and a differential probe (CH4). Screenshots and waveform of tests was saved using the usb-port in the lower left corner. The front panel of the oscilloscope is shown in figure 16.

Figure 16 - Front panel of oscilloscope Tektronix MSO 2024B

3.3 Software

The FPGA board runs a program designed by SINTEF Energy Research, where two of its functionalities are single pulse testing and double pulse testing. The functions that have been used during these tests are summarized in table 2. A full explanation of all functions on the program are found in appendix A.

Table 2 - FPGA-program software description

Function code	Value (ps / pd)	Comment
ps	"Single pulse"	Activates single pulse
pd	"Double pulse"	Activates double pulse
r	"read"	Prints status
sta	"start"	Starts switching
sto	"stop"	Stops switching
t1	0 / 7 µs	Length of first double pulse test
t2	0 / 280 µs	Length between first and second pulse
t3	10 µs / 7 µs	Length of single pulse or second double pulse
t4	5 s	Time between each main switching scenario
AL	Q	Activate connected gate-channel to switching

3.4 Test Plan and Different Liquids

The setup will be submerged in two different insulating liquids, in 14 days each, with an air test as a reference. The first test is to run a 3.62 kV single pulse in 10 µs, which corresponds to turn-off at approximately nominal current of the IGBT (125 A). The second test is to run a double pulse test at 3.62 kV, where both on-periods are 7 µs and the off-period between the pulses is 280 µs, corresponding to a turn-off at nominal current.

The first liquid is MIDEL 7131. It is today used in thousands of new transformers and theoretically a very qualified dielectric liquid for subsea use. It can absorb large amounts of water without reduction of the breakdown voltage and can operate in both high and low temperatures. It is also fully biodegradable. More information on MIDEL 7131 can be found in its product guide and technical datasheet [17, 18].

Temperature and moisture-levels are important to monitor during tests, and the temperature will be kept as constant as possible throughout all tests. The moisture level will at first be kept at approximately 5 % in MIDEL, which is the low point of the relative moisture levels for Infineon IGBTs in air, defined by IEC 60721-3K3. If components are working at this moisture level, then test at higher temperature and elevated moisture levels can be performed. All components will be washed in isopropanol between each liquid. Tests using preconditioned IGBTs, with custom made silicone gel or high moisture gel/liquid can also be performed.

The second liquid is Galden HT230. It has excellent dielectric properties which makes it very suitable for semiconductors and electronic-industries. The liquid has a low viscosity, is nontoxic and have a high resistance to thermal degradation. It has a large operating temperature-range. More information on Galden HT230 can be found in its product guide and technical datasheet [19, 20]. Tests using Galden will be performed at a humidity-level of 25 % RH which is how product is delivered from the manufacturer.

4 Overview of Safety Functions

The whole test setup has been built from scratch during this master thesis. Safety has had a high priority since both high voltage and charged capacitors can be lethal if handled incorrectly. Kjell Ljøkelsøy at SINTEF Energy Reserach has been of great help on a consultative basis when designing a safe test setup, and is also the chief of security on the test-cell (LFS). A risk assessment has been performed in co-operation with Halsten Aastebøl at NTNU. After the setup was completed, a thorough review of the setup was performed by Arne Petter Brede from SINTEF Energy Research and Bård Almås from NTNU. The main safety-functions are further described in this chapter.

4.1 Cabinet

The complete test setup is enclosed inside an earthed cabinet. This ensures that the whole setup is protected and no physical interaction is possible when the cabinet is closed. Inside the cabinet the high voltage and low voltage wiring has been separated into two different zones. The cabinet and the different zones are shown in figure 18. A large plexiglass is mounted on the front door for observation purposes.

4.2 Door Sensor

The power is automatically disconnected if the front door is opened. When the cabinet is without power, the capacitor will be discharged through a discharge resistor within 1 second. This will ensure that no one can come in contact with any high voltage equipment at any time. The door sensor is shown in figure 17.

Figure 17 - Door sensor

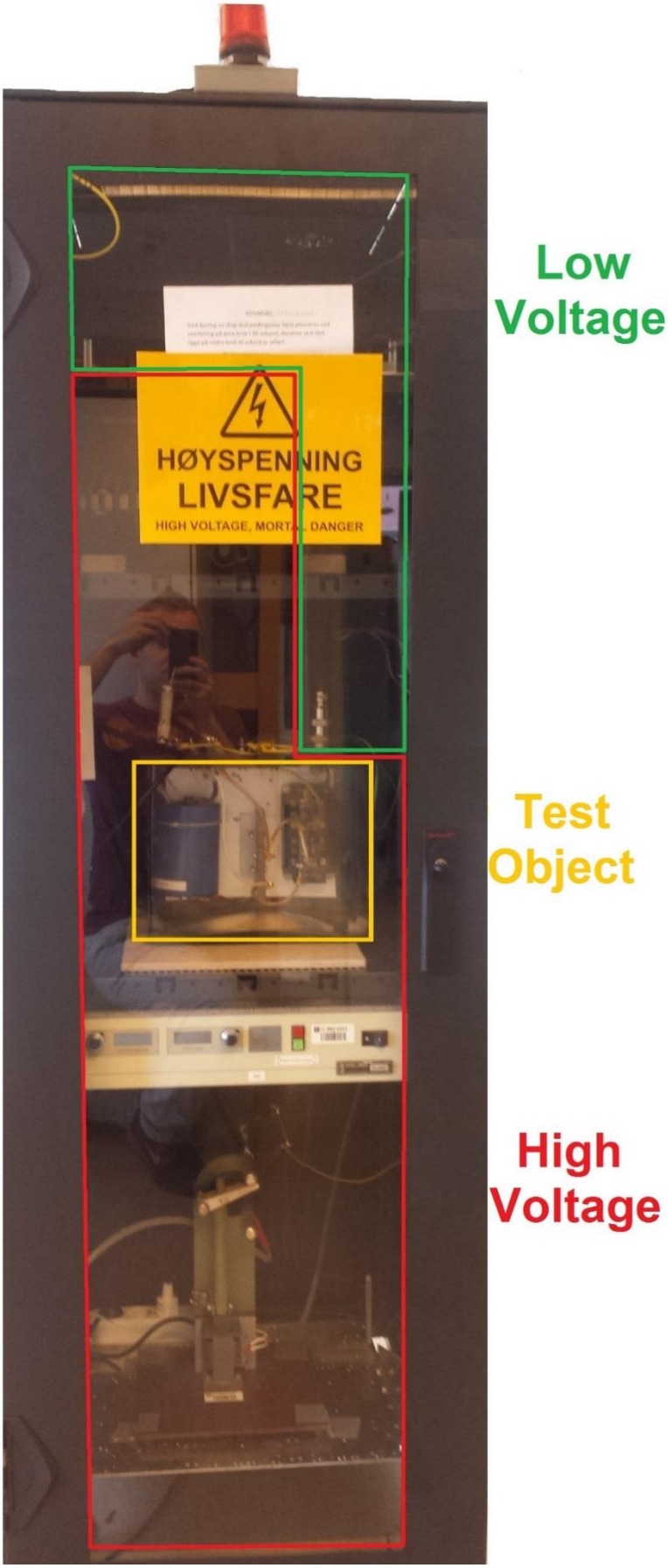

Figure 18 - Test setup enclosed in cabinet including voltage-zones

4.3 Remote Control

Outside the cabinet, at the control and measurement station, it is located a green “high voltage on” button and red emergency stop button. No high voltage can be present unless the cabinet is closed, and this green “high voltage on” button is pressed. The capacitor will also be connected to earth at all times unless this high voltage button is pressed, ensuring that there is no energy stored in the capacitor when equipment is off. A high voltage relay will automatically switch the capacitor to the high voltage source when the green button is pressed, charging the DC-link. This relay needs active power to be operative, so in case of power failure, the capacitor will be discharged through resistors via this relay. In figure 19 the green and red button are shown, including one of the warning lights.

Figure 19 - Remote control and emergency button

4.4 Warning Lights

Two warning lights are used in the setup to indicate that high voltage is turned on. The first is the small light shown in the upper left corner in figure 19. The second is a larger light put on top of the whole cabinet. This can been seen in the upper part of figure 18.

4.5 Earthrod and Extra Discharge Resistor

A custom made earth rod is hung inside the cabinet. This is used to manually ensure that the capacitor and the rest of the test equipment is properly grounded when working on any of the equipment. A step-by-step approach on how to open the cabinet and connect the earthrod is posted outside the test-cabinet.

An extra manual discharge resistor is mounted on the positive capacitor connection. This is done in case something fails with the automatic discharge resistor to still ensure a safe discharge of the capacitor. Both the earthrod and spare discharge resistor is shown in figure 20.

Figure 20 - Earthrod and spare discharge resistor

5 Pre-characterization of Test Components

Before any of the critical test-components were submerged in liquid, a pre-characterization of the components were performed. The test were done in air, at approximately 25 degrees Celsius. The complete test-setup is then also tested and characterized. This will ensure that changes due to the insulating liquid should be observed.

5.1 IGBT Module

Infineon AG is the manufacturer of the IGBT modules used inn all the tests. It is a custom made test object based on the commercial module FZ250R65KE3. The standard module consist internally of two base substrate which are paralleled to increase the current rating. In the custom built, the two substrates are disconnected from each other, creating two completely separated IGBTs inside one module. The current rating of each IGBT is then reduced to 125 A, half of the rated current on the standard module. Figure 21 illustrated the modification of the module. IGBT-module denoted as #1 has serial number 70008769_26, while module #2 has serial number 70008769_23. The gate-oxide layer is very sensitive to static charges. It is therefore important to keep gate-emitter short-circuited unless it is connected to the gate driver.

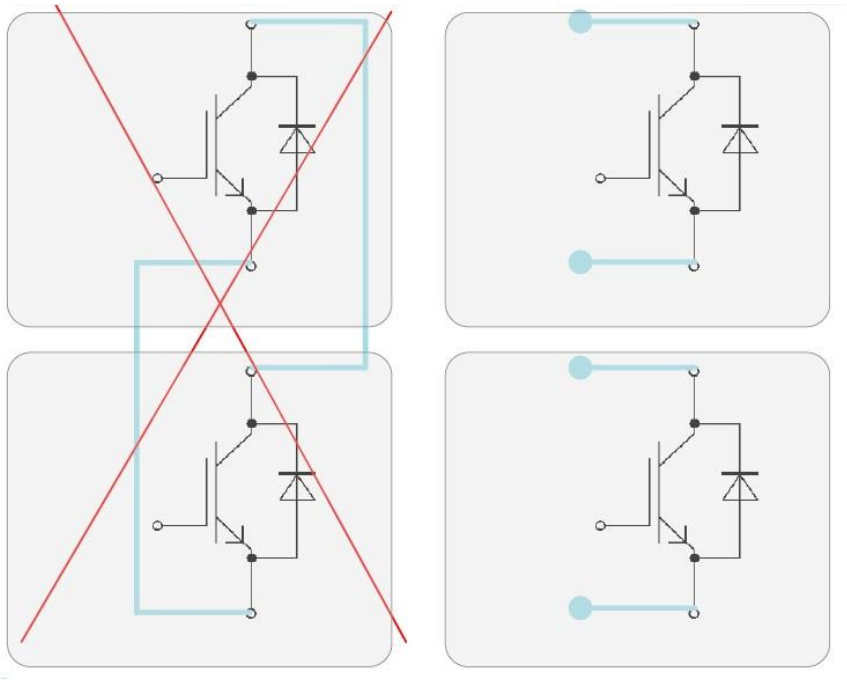

Figure 21 - Illustration of module modification [8]

When the IGBT module has been split in two different IGBTs, a definition of the IGBTs are necessary. This is done using the layout of the contact-points on the IGBT-module. The definition is according to figure 22.

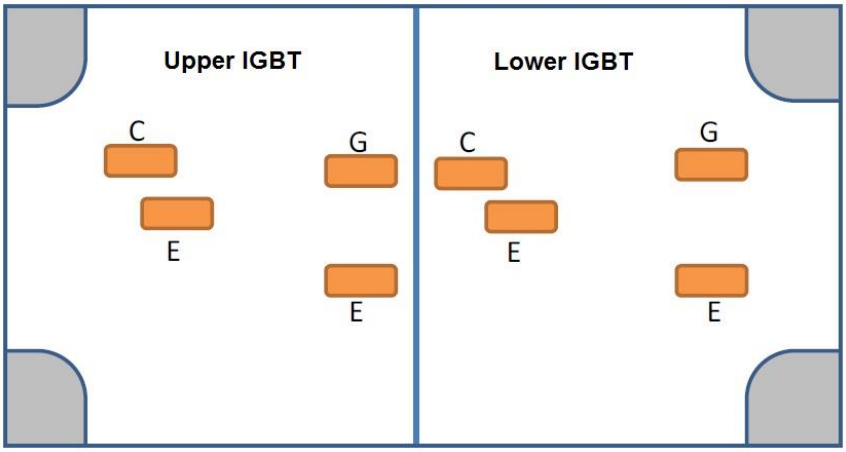

Figure 22 - Definition of the IGBTs in the IGBT module [8]

5.1.1 Visual Inspection

The lid of the modules has been removed so that the insulating liquids will cover all open areas during testing. Figure 23 show IGBT #2 prior to testing.

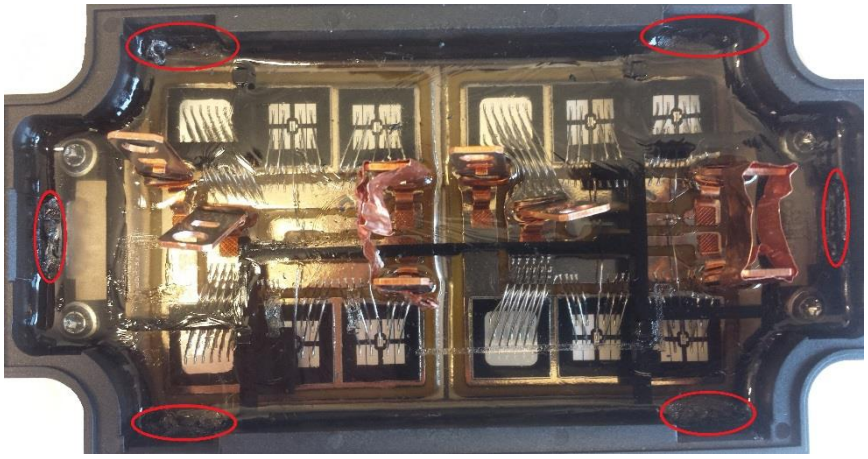

Figure 23 - Picture of IGBT module #2

The IGBTs were similar after lid-removal, therefore figure 23 is used as reference for both modules. The gel is initially transparent, and covers chips and wire bonds. Small marks on the gel is observed and shown in the red circles in the figure. They are caused by the removal of the top lid. The gel is filled up exactly to the point where the four plastic support-pins are covered, and will be indicators for any swelling after the tests. A small increase in the gel-height is observed close to the connection pins.

5.1.2 Blocking Voltage Test

In this test, the gate-emitter of the IGBT is short-circuited, thereby setting the IGBT in blocking-mode. The IGBT is then tested up to its rated collector-emitter blocking voltage and the leakage current is measured. For this test, the upper and lower IGBT is tested separately. The wiring diagram for the test is seen in figure 24.

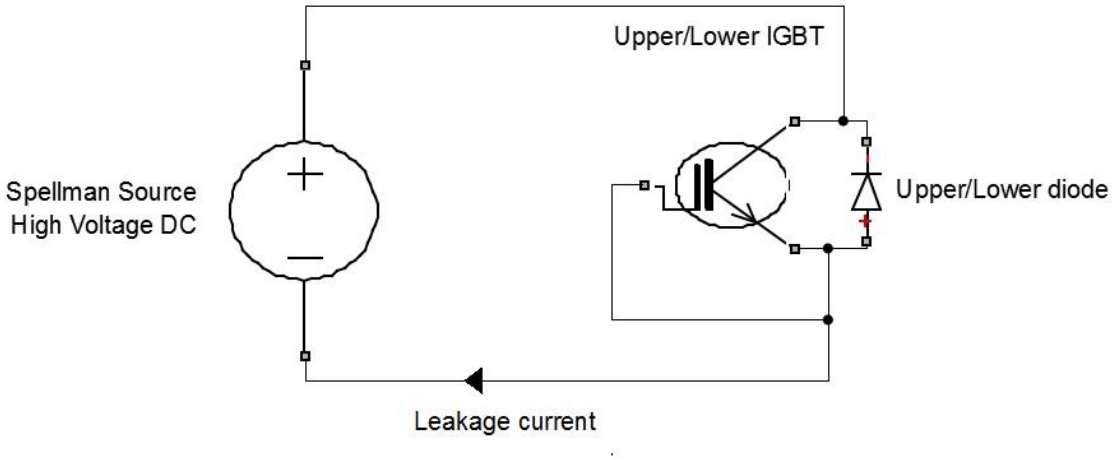

Figure 24 - Wiring diagram for blocking voltage test

The test was performed at 6.5kV and the results are shown in table 3. The highest leakage current was 13.5 µA on lower IGBT #2. The datasheet has a maximum ”Collector-emitter cut-off current” at 5.0 mA, meaning that all the IGBTs are well within rated values [11].

Table 3 - Results for the blocking voltage test

IGBT Module #	Voltage (Collector-Emitter)	Leakage Current (Upper / Lower)
1	6.5 kV	7.7 µA / 8.4 µA
2	6.5 kV	10.0 µA / 13.5 µA

5.1.3 Forward Voltage Test

This test uses an instrument at SINTEF Energy Research called DM 659 and is specifically designed for measuring forward voltage drop on semiconductors. The gate voltage is set to its nominal voltage, then a controlled current pulse is passed through the collector-emitter while measuring the forward voltage drop. The results is shown in table 4 and figure 25. The results at rated current (125 A) is close to the typical forward voltage drop of 3.00 V, given in the

datasheet [11]. This test is only performed on the lower IGBT on the module, since this is the IGBT that will be actively switched in liquids.

Table 4 - Forward voltage drop results

Lower IGBT Module #	Current I_{ce}	Forward voltage drop V_{ce}
1 / 2	10 A	1.526 V / 1.537 V
1 / 2	20 A	1.782 V / 1.798 V
1 / 2	30 A	1.967 V / 1.986 V
1 / 2	40 A	2.121 V / 2.142 V
1 / 2	50 A	2.255 V / 2.279 V
1 / 2	60 A	2.380 V / 2.405 V
1 / 2	70 A	2.496 V / 2.523 V
1 / 2	80 A	2.605 V / 2.634 V
1 / 2	90 A	2.711 V / 2.741 V
1 / 2	100 A	2.813 V / 2.844 V
1 / 2	110 A	2.912 V / 2.944 V
1 / 2	120 A	3.007 V / 3.041 V
1 / 2	125 A	3.054 V / 3.088 V

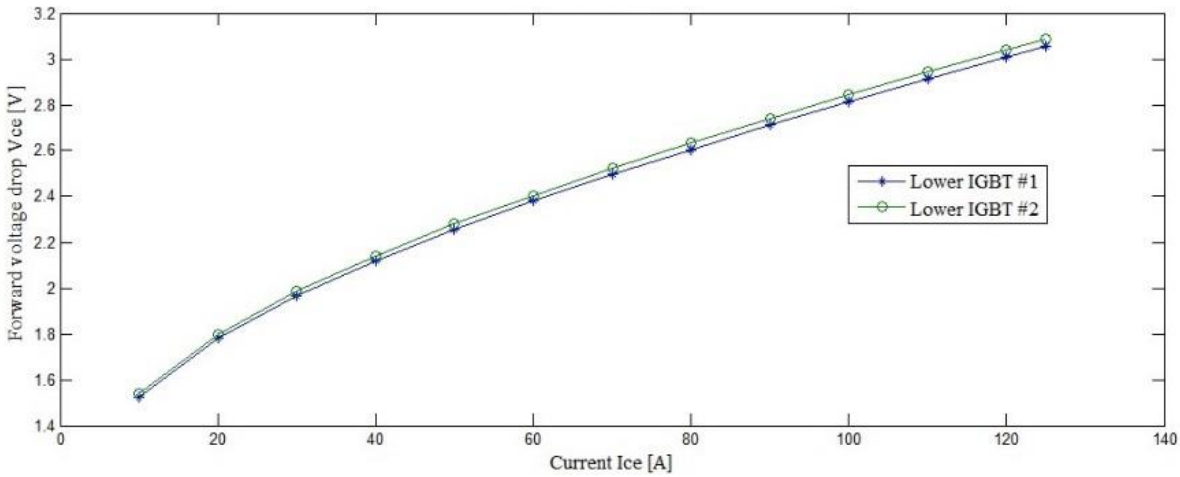

Figure 25 - Trend of the forward voltage drop versus the collector current

5.1.4 Gate Threshold Voltage Test

An adjustable low voltage DC-source is connected to provide the same voltage potential across gate-emitter and collector-emitter on the IGBT. The voltage is increased until a collector current of 10mA is reached. The voltage on the DC-source is then measured using a voltmeter. The wiring diagram for this test is shown below. The upper and lower IGBT is tested separately.

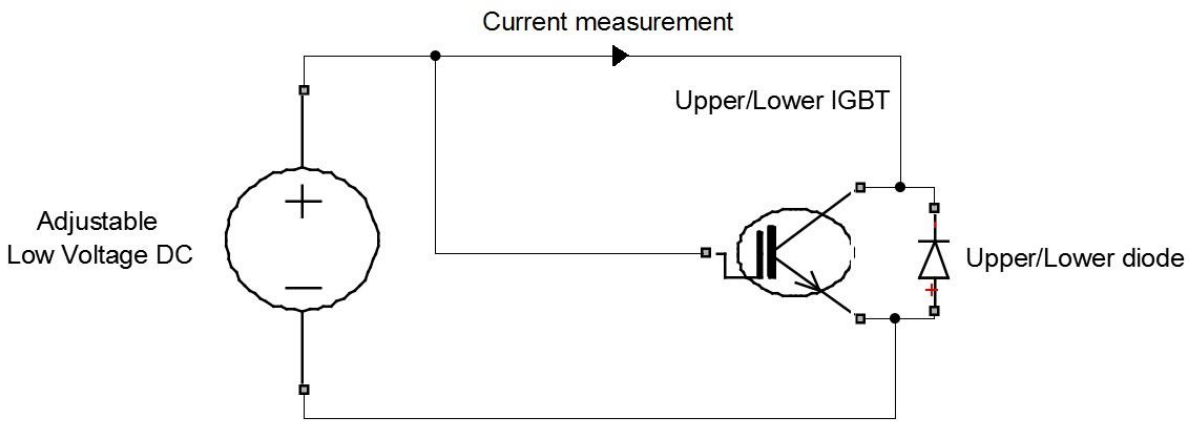

Figure 26 - Wiring diagram for gate threshold voltage test

A small increase past the gate threshold voltage will quickly increase the collector-current up to the current-limit of the voltage source, since passing the threshold voltage will turn on the IGBT. The voltage is increased slowly and a current-limit of 20 mA is set on the voltage source. The results is shown in table 5. The minimum and maximum-values for a gate threshold voltage test with collector-current of 35 mA are in the datasheet given at 5.4 V and 6.6 V. This is when the IGBTs upper and lower part is paralleled, meaning that the test-value collector-current of one IGBT is equal to 17.5 mA. The test was however performed at 10 mA, due to comparison-reasons from an earlier test-result performed by SINTEF Energy Research. The difference from using 10 mA or 17.5 mA as the threshold current is very small, therefore the values can be directly compared with the values given in the datasheet. The measured values are well within specification in the datasheet.

Table 5 - Results for the gate threshold voltage test

IGBT Module #	Collector-Emitter current	Applied voltage (Upper / Lower)
1	10.00 mA	5.895 V / 5.905 V
2	10.00 mA	5.924 V / 5.917 V

5.2 DC-link Capacitor

The DC-link capacitor used in the tests are a metallized polypropylene capacitor from Electricon. It is a custom made capacitor, based on the E51-series that Electricon delivers. This is a capacitor with a very good ratio of capacitance to volume, a high pulse strength and good self-healing characteristics. The customization compared to a standard E-51 series is that it has not been filled with resin, hence the insulating liquid will be in direct contact with the film inside the casing. The test object is a 5 µF /6.75 kVDC capacitor element, and has the special article number E51.P12-502R20. A datasheet for the capacitor is not available since it is custom made, but an overview of its most important characteristics are given in table 6.

Table 6 - Overview of capacitor characteristics

Rated Capacitance	5 µF
Rated DC-Voltage	6750 V
Max ripple current	~50 A
Diameter element / casing	78 mm / 90 mm
Length element / casing	76.5 mm / 125 mm

A photo of the capacitor-element including the casing is shown in figure 27.

Figure 27 - Capacitor element, casing and top/bottom lid

5.2.1 RLC-measurement of Capacitor Element

The capacitance and Θ-angle were measured using a RLC-meter. (Fluke PM306). Changes due to being exposed to the insulating liquid can then be examined after the high voltage switching tests. The results from the RLC-meter are shown in table 7. The measuring-equipment is not able to measure any losses in the capacitor at 50 Hz due to the large capacitance to resistance-ratio.

Table 7 - Results of RLC-measurement on capacitor

Test frequency	Capacitance	Θ - angle
50 Hz	4.8923 µF	-90.0 °
1000 Hz	4.8927 µF	-89.9 °

5.2.2 Leakage Current Test

A leakage current test at nominal voltage was planned, but did not give reasonable results due to inaccurate test-equipment. Further explanation and attempts to solve this problem is described in chapter 6.5.

5.3 Concept Gate Driver

The commercially available 2SC0535 SCALE-2 driver core and the 2BB0535T base board from Concept has been used. It is a dual channel driver with isolated power and signal transfer to the secondary stages by magnetic transformer [21, 22]. The driver assembly is shown in figure 28.

The gate driver has both electrical and optical interface. Only the optical interface will be used, as the electrical has been tested in insulating liquid by SINTEF Energy Research in earlier research. Since optical interface is used for communication, only power and no control signal will be supplied through the ribbon cable connection. This gate driver has several protection-mechanisms, including dynamic advanced active clamping, short-circuit protection and supply undervoltage detection.

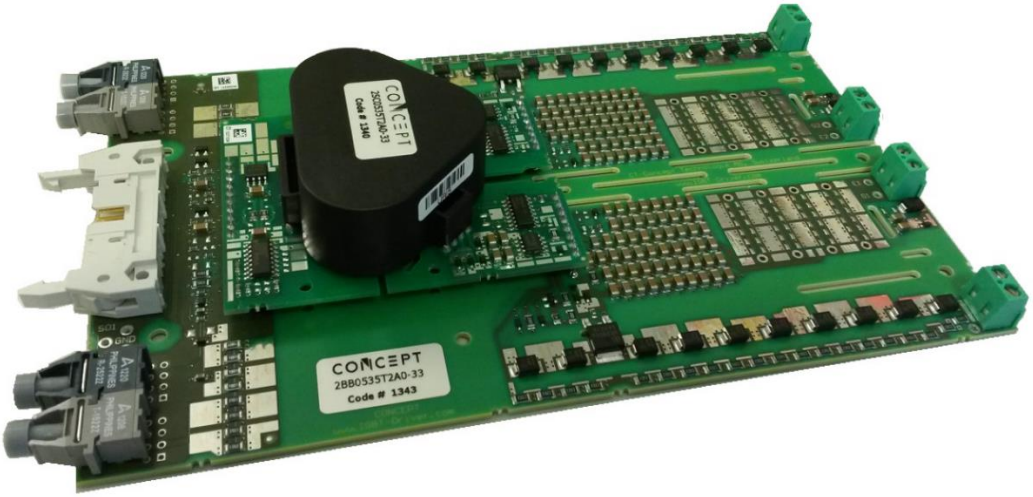

Figure 28 - Gate driver core and base board

When using the optical connection on the gate driver, an interface card is needed to transform the electrical signal from the FPGA-board to optical trigger signals. This second interface card is put in liquid together with the concept driver. It has one optical connection for fault signal and one that controls the switching. The schematics for the interface card #2 is presented in appendix B. The optical interface card can be seen in figure 30.

The main test for these two cards is functionality and observation of any large changes in gate driver output. Compatibility of optical interface in liquids are an important factor, since liquids have different refractive index profiles and can affect the fibre-optical communication link.

6 Test-setup Modifications

During construction and testing of the cabinet and test equipment, several issues arose. The main problems and modifications are discussed in this chapter. The issues described in chapter 6.1 is an important result related to fibre-optical communication in MIDEL.

6.1 Gate Turn-on Delay in MIDEL

After the test-setup was submerged and vacuumed in MIDEL, a signal-delay were observed at the gate driver output. The peak turn-off current varied from 100 A to 130 A using a 10 µs single pulse and DC-voltage of 3.62 kV. This observation was investigated further by comparing the turn-on signal from the FPGA-board to the turn-on output from the gate driver.

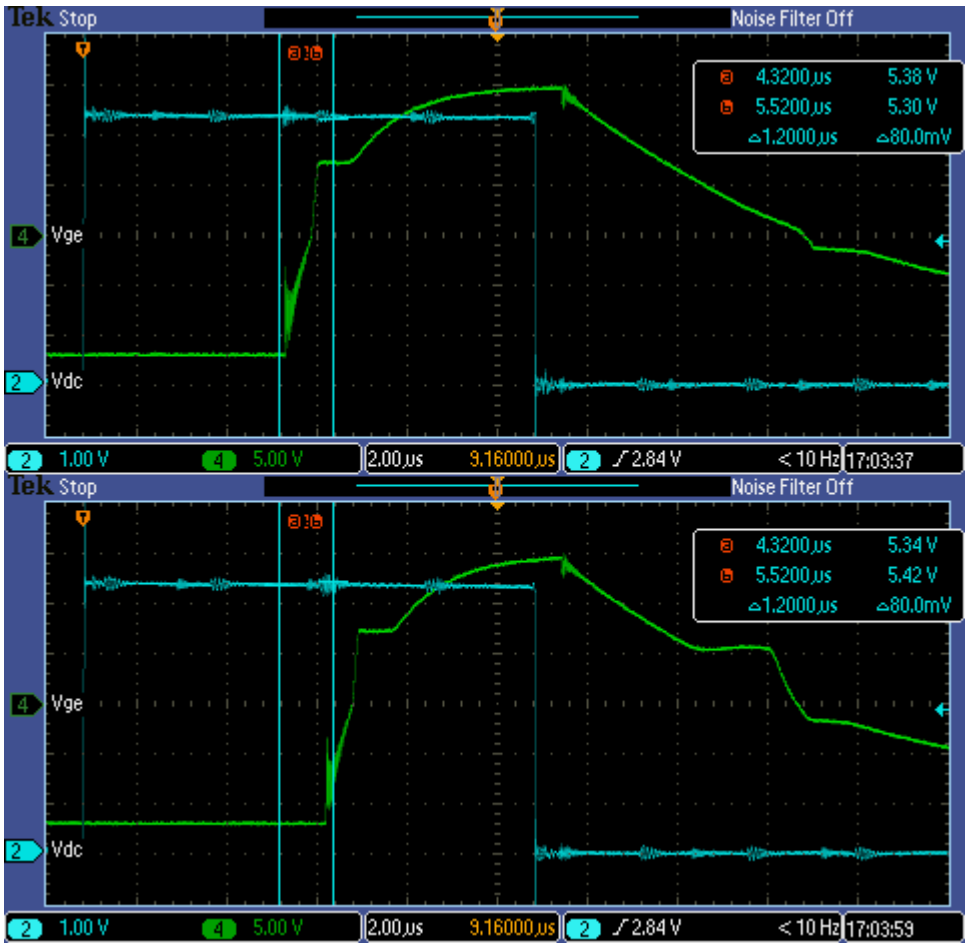

Figure 29 - Turn-on delay on the gate driver (Green) while submerged in MIDEL

In figure 29 a disparity between two turn-on signals is found and a turn-on delay up to 1.2 µs is observed. The turn-on from the FPGA is constant (Blue), and turn-off moment is constant on the gate driver. This indicates that the turn-on signal is delayed due to a too weak turn-on light in the fibre-optical sender. The datasheet for the HFBR1528 fibre-optical sender was examined.

Test-setup Modifications

In appendix B, the wiring diagram for the optical interface is included. The surface-mounted resistors R11 and R14 on interface-board #2 were reduced from 47 Ω to 33 Ω, thereby increasing the power in the optical sender to peak power according to the datasheet [23]. The two replaced resistors are shown in the red square in figure 30. The increase from nominal to peak power should not result in any problem in pulse-testing. Testing afterwards confirmed that any variation in signal-delay was gone.

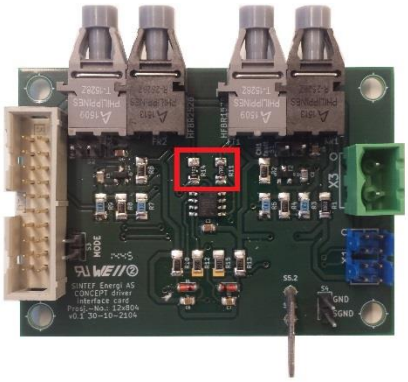

Figure 30 - Optical interface card

During the test in MIDEL and Galden, a small decrease in peak current at turn-off was observed. This could be a result of the fibre-optical communication. A small constant delay due to the liquid would result in a smaller peak current. After the Galden test, the complete setup was rinsed in isopropanol. The setup was then tested and compared to the air-reference, both with the optical fibre that was exposed to MIDEL and Galden, and with a new fibre-optical cable. A small increase of peak turn-off current was observed after replacing the cable. This can indicate that the modification only stabilized the delay, and did not completely remove it. Some liquid could have penetrated the fibre-optical cable resulting in this delay, while some could be stuck at the transmitter- and receiver lens. An overview showing the changes is shown in table 8.

Table 8 - Changes in single pulse peak-current from optical communication delay

Surroundings	Air Reference	MIDEL	Galden	Air Cleaned	Air New fibre
Peak turn-off current	133 A	128 A	125 A	127 A	129 A

6.2 LEM-shunt, Rogowski-coil or Current-probe

Initially, the plan were to use a LEM-shunt, which was the only solution that enabled current-measurements inside the container of liquid. SINTEF Energy Research had earlier tested a LEM-shunt in pressurized MIDEL, and the exact same shunt was considered to measure the emitter current in this test-setup. The LEM-shunt is an off-the-shelf LA 205-S, with capacitor-modification to withstand liquid and pressure. An electrolytic capacitor was changed to a tantalum capacitor with the same rating, and proper performance was verified by SINTEF Energy Research. It was mounted on the same test-plate as the IGBT, and the return connection from the lower IGBT-emitter went through the LEM-shunt measurement area on the way back to the Spellman-source (Ground). This solution was also the one that would ensure as low as possible loop-inductance, minimizing voltage overshoot at turn-off.

In the first air-tests a Rogowski-coil (PEM CWT 3R 600A) was used in the same loop to verify the LEM-shunt measurements. The Rogowski-coil was then placed at the same emitter-current loop next to the LEM-shunt. The results from a 10 µs single pulse test at 500 V is shown in figure 31. The LEM-shunt has large disturbances/oscillations in the current-measurements, but the linear increase and maximum-value in the switching-interval is similar to the Rogowski-coil.

Figure 31 - Emitter current: Rogowski-coil (Yellow) vs LEM-shunt (Purple)

Test-setup Modifications

A modification to the top-plate was performed to increase accuracy on the emitter current measurement. This was done by connecting the emitter from the lower IGBT to a very small current loop on the upper side of the test-plate. The loop would then let the Rogowski-coil be able to measure the emitter-current without being exposed to the insulating liquids. The loop was made very small to minimize the voltage overshoot at turn-off.

A Tektronix current probe (TCP0150 150A-pk) was used to verify the performance of the Rogowski-coil, and if possible, improve turn-off accuracy. This did not result in any improvements, as the current probe had a small oscillation at the end of the turn-off time. A closer look at the turn-off measurement troubles and comparisons of current probe and Rogowski-coil is shown in figure 32. This figure is also a good illustration of the different turn-off segments discussed in chapter 2.1.2. It can clearly be observed where the MOSFET turn-off ends and the BJT current-tail continues.

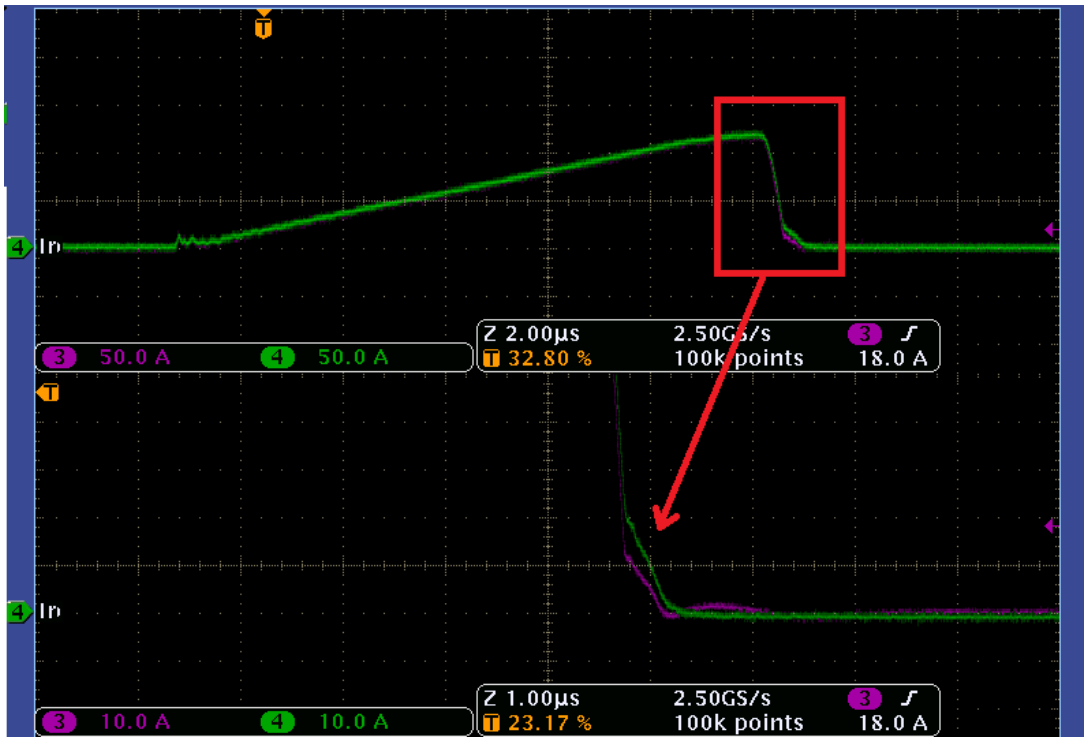

Figure 32 - Emitter current: Rogowski-coil (Green) vs Current-probe (Purple)

6.3 Signal Noise on Gate Driver Output

The first setup gave very large noise-oscillations when measuring the output signal of the gate driver. A normal voltage probe was used, and the wiring for the measuring-point was twisted together with the signal-wiring for the gate driver and Sensirion-sensor. The results of a 10 µs single pulse before modifications are shown below.

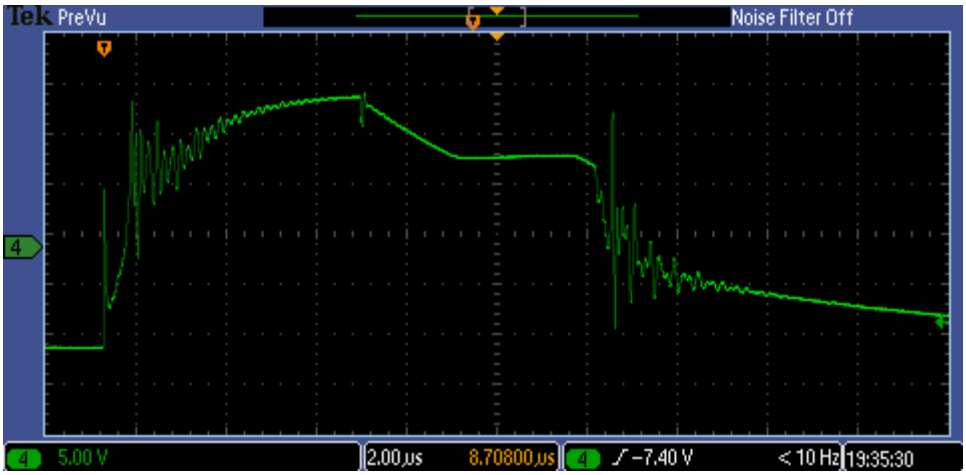

Figure 33 - Initial signal noise on gate driver output

To reduce the oscillations, a differential probe was introduced instead of the normal voltage probe. The cable-lengths for measuring was cut down to its minimum, and separated from the other signal cables. Only the differential probe wires was put inside the cabinet. These combined actions resulted in the lowest obtainable signal noise on the gate driver. The improvement can be seen in figure 34.

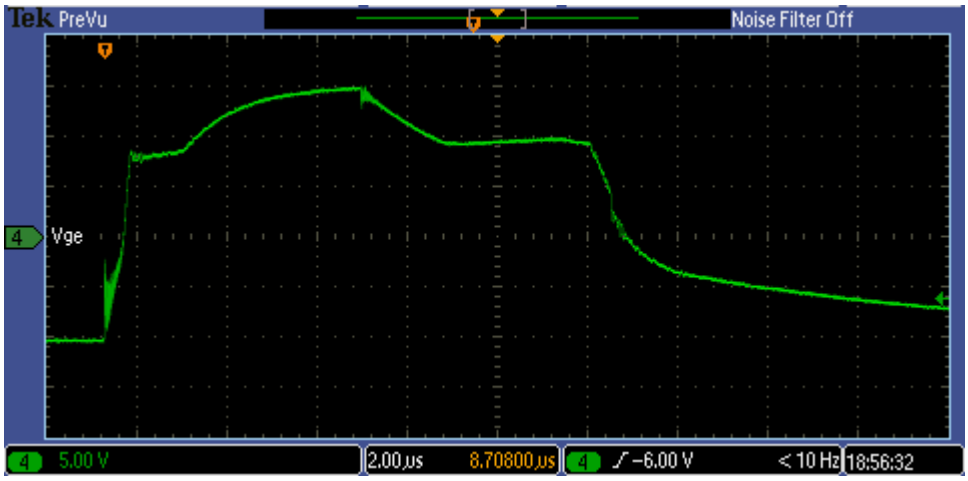

Figure 34 - Improved signal noise on gate driver output

6.4 Calibration of High Voltage Probes

When the first switching test of the setup was performed, a large negative voltage was measured across the IGBT during its on-period. The test was done at approximately 1 kV DC-link value. According to the forward voltage test performed in chapter 5.1.3, a voltage between 1-3 V should be measured depending on the current going through the IGBT. In figure 35, a voltage between negative 300 to negative 600 V was measured during the IGBTs on-period.

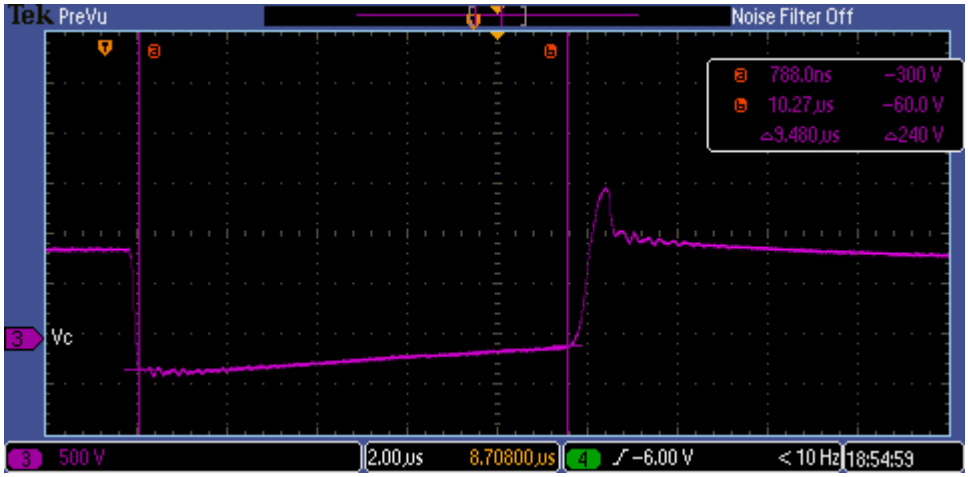

Figure 35 - Uncalibrated high voltage probe

The high voltage probes was checked using the square wave output on the oscilloscope. A large deviation from the desirable square wave was measured. The calibration screw on the probes was then adjusted, resulting in much more accurate measurements. Both high voltage probes was calibrated. The high voltage probes is however not accurate enough to give the exact forward voltage of the IGBT. In figure 36 a measurement at 3.3 kV show a great improvement after calibration.

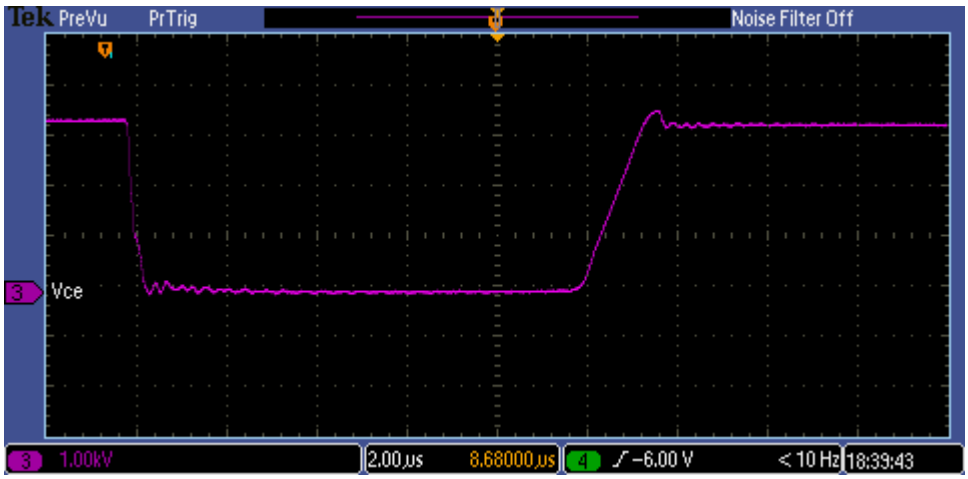

Figure 36 - Calibrate high voltage probe

6.5 Leakage Current Measurement of Capacitor

Measuring the leakage current in the capacitor could be used as an indication for any changes due to the different liquids it is submerged in. An increase in leakage current is often an indication towards breakdown or failure.

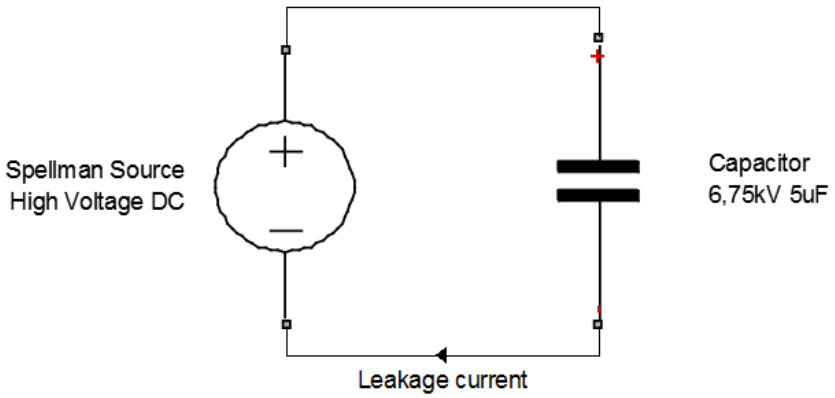

Figure 37 - Wiring diagram for capacitor leakage current

The wiring diagram in figure 37 illustrates how this test was performed. However, during this test, the capacitor was charged to 6.5 kV, and a negative leakage current was measured, meaning current flowed into the high voltage source. Large pulses of high current in positive direction was observed every other second. This was further investigated, and the conclusion was that the Spellman source do not have an accurate output. It charges the capacitor up to 6500 V, and the capacitor starts to deliver a small current to the source. The voltage on the capacitor drops gradually. After a few seconds, the voltage has dropped down to the point where the source measures the voltages to be one digital step lower than 6500 V. It will then recharge the capacitor up to 6500 V. An analogue high voltage source, or with a much more accurate analogue to digital conversion of the voltage output is therefore needed to performed this test.

A workaround of this problem was tried using a series of resistors in parallel to the capacitor, which was assumed to force the Spellman to deliver a constant current to the resistance, and then fix the voltage output. This did however not work, as it only resulted in higher current-pulses from the voltage source every other second.

7 High Voltage Liquid Results

This chapter includes all results from single and double pulse testing in air, MIDEL and Galden. The tests was performed in the different liquids as explained in chapter 3.4. Table 9 summarize the maximum values during the 10 µs long single pulse test with a DC-link of 3.62 kV. "Peak turn-off current Emitter" is the current at the instant the IGBT turns off, which is when the current is the highest. "Voltage overshoot Collector-Emitter" is the overshoot created at turn-off, since current-decrease is present. "Turn-off time" is the time the IGBT uses to go from maximum to zero current.

Table 9 - Single pulse result overview

Surroundings	Peak turn-off current emitter	Voltage overshoot Collector-Emitter	Turn-off time
Air, 23 °C 31 % RH	133 A	3820 V	696 ns
MIDEL, 23 °C 5.3 % RH	128 A	3800 V	632 ns
Galden, 24 °C 25.8 % RH	125 A	3840 V	640 ns

A summarizing of the double pulse test results is provided in table 10table 1. All the double pulse tests are performed with 3.62 kV DC-link, 7 µs time for both pulses (t_1 & t_3), and a pause between the pulses at 280 µs (t_2). The pause between the two pulses was defined in air as the pause that gives a maximum turn-off current equal to the nominal current capacity of the IGBT at 125 A.

Table 10 - Double pulse result overview

Surroundings	Peak turn-on current emitter	Peak turn-off current emitter	Voltage overshoot Collector-Emitter	Turn-off time
Air, 23 °C 31 % RH	255 A	125 A	3800 V	582 ns
MIDEL, 23 °C 5.3 % RH	246 A	122 A	3780 V	610 ns
Galden, 24 °C 25.8 % RH	239 A	119 A	3720 V	614 ns

High Voltage Liquid Results

The complete double pulse test in air is shown in figure 38. This is how the double pulse test was performed in all the surroundings. The results of the first pulse in the double pulse test will not be included, as it will be the same as a single pulse test, only with a shorter period. Therefore the second pulse is the only pulse presented in the results of the double pulse test. This is the area shown inside the red square in figure 38. Waveforms and screenshots of turn-on and turn-off pulses are stored for analysis. There is a fairly long off-period between the first and second pulse to ensure that the second turn-off current of the IGBT is kept below/close to nominal values. Pulse testing was performed each third day during the 14 day period and the results showed no major changes when exposed to either MIDEL or Galden.

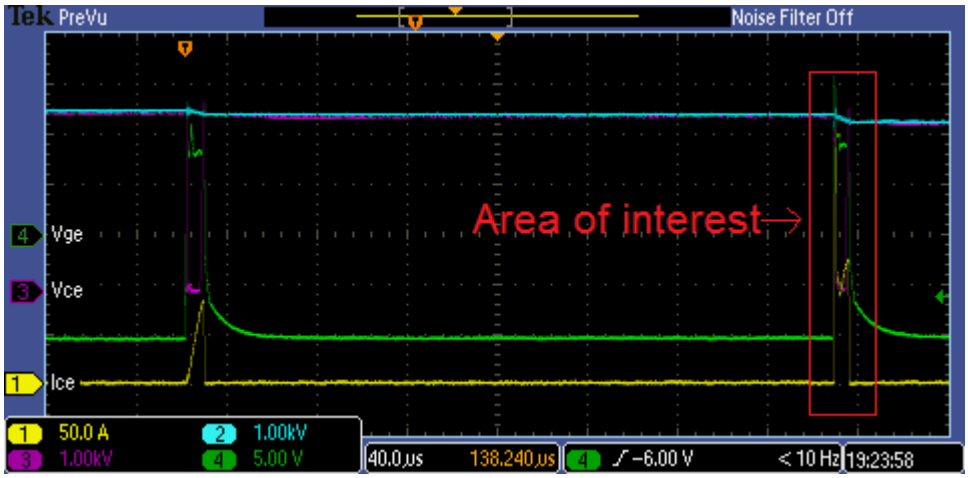

Figure 38 - One double pulse test

A high voltage blocking test in both liquids was performed before each pulse test. This was done with the IGBT in blocking mode. The voltage was increased gradually to 6500 V. No breakdown occurred in any of the liquids. The components did not give any signs of failure. No irregular sounds were heard during these tests.

7.1 Results from Single Pulse Testing

The screenshot from the oscilloscope on the single pulse tests performed is shown in figure 39. Both MIDEL and Galden had successful results, meaning they gave similar results as the reference test in air.

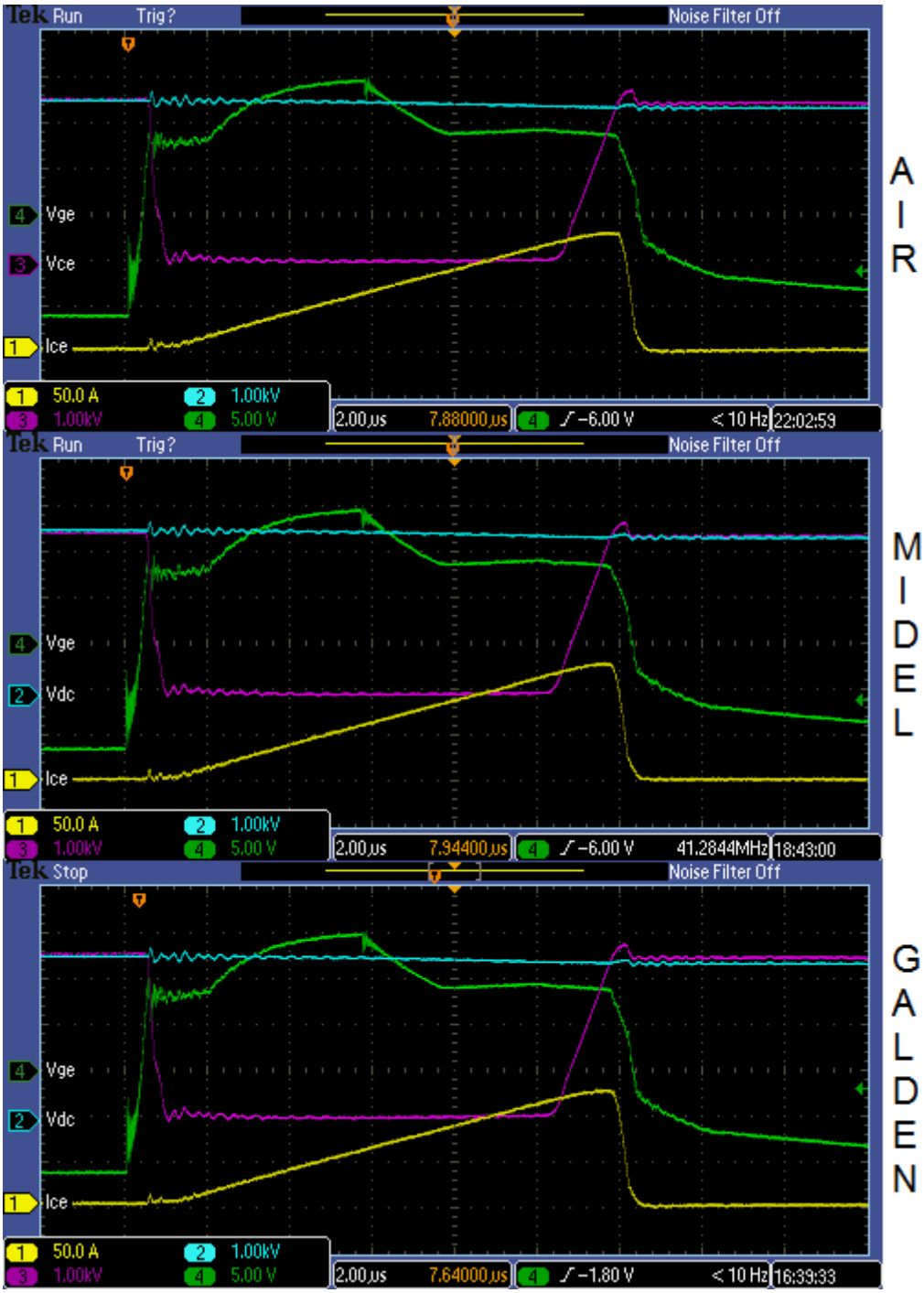

Figure 39 - Screenshot of 3 single pulse tests

7.2 Results from Double Pulse Testing

The screenshot from the oscilloscope on the double pulse tests performed is shown in figure 40. Both MIDEL and Galden had successful results, meaning they gave similar results as the reference test in air.

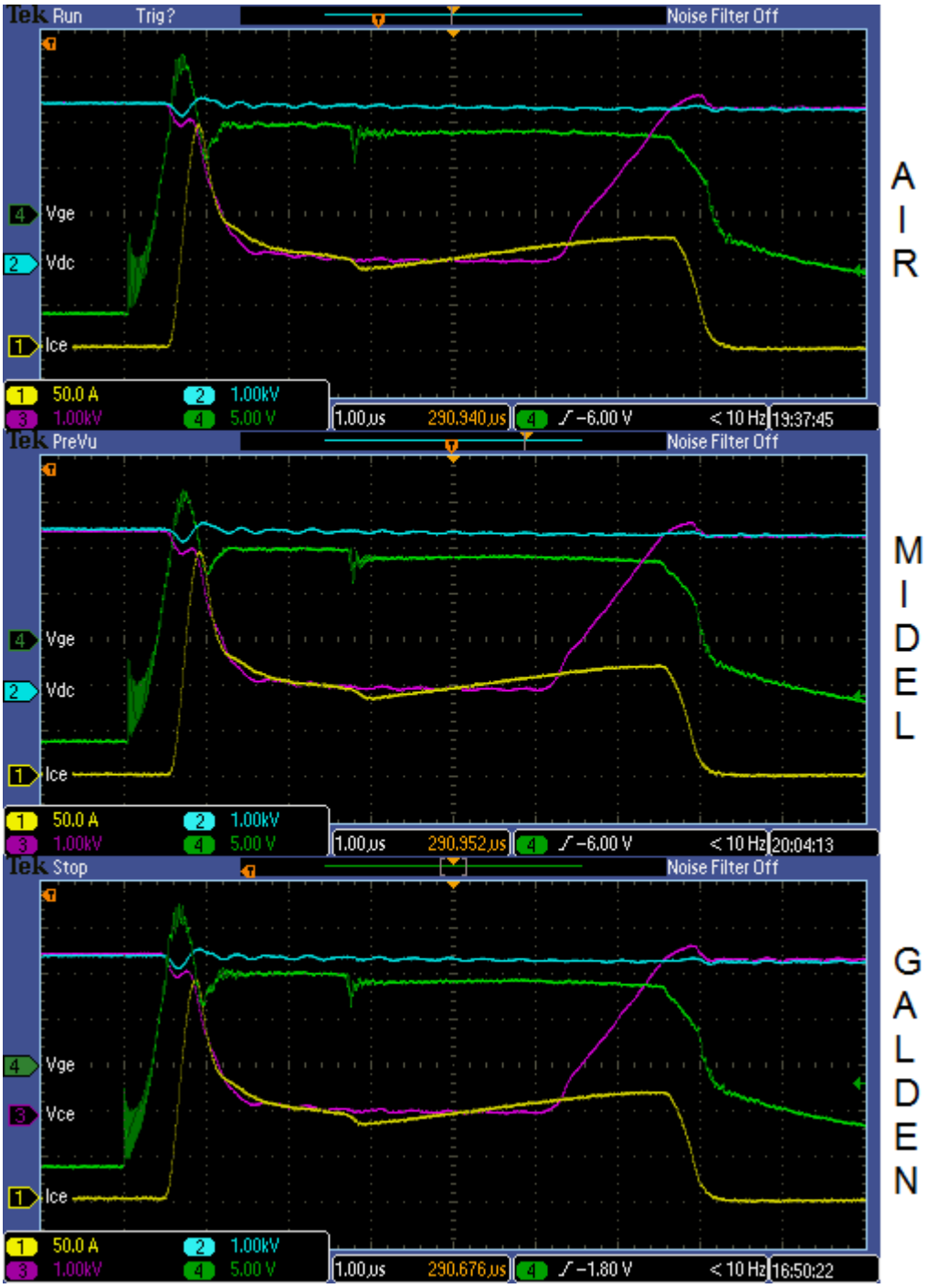

Figure 40 - Screenshot of 3 double pulse tests

8 Post-characterization of Test Components

All the tests performed are described in chapter 4. Only the test-result from the post-characterization will be given in this chapter.

8.1 IGBT Module

IGBT #1 was exposed to the MIDEL-liquid in 14 days and successfully switched at 3.62 kV several times during this period. IGBT #2 was exposed to the Galden-liquid for 14 days and switched successfully at 3.62 kV several times during this period. The results from the three different test performed on the IGBTs showed that no changes had happened to the IGBTs after liquid exposure.

8.1.1 Visual Inspection

Both modules where rinsed in isopropanol after being exposed to the liquids for 14 days each. IGBT module #1 is shown in figure 41. There is no clear sign of degradation of the gel. The same lid marks are observed. The gel does however show a very small indication of swelling. An increased unevenness of the gel-height is observed close to the connection pins. Module #2, which was exposed to Galden, was exactly the same as before exposure, with no signs of degradation or swelling.

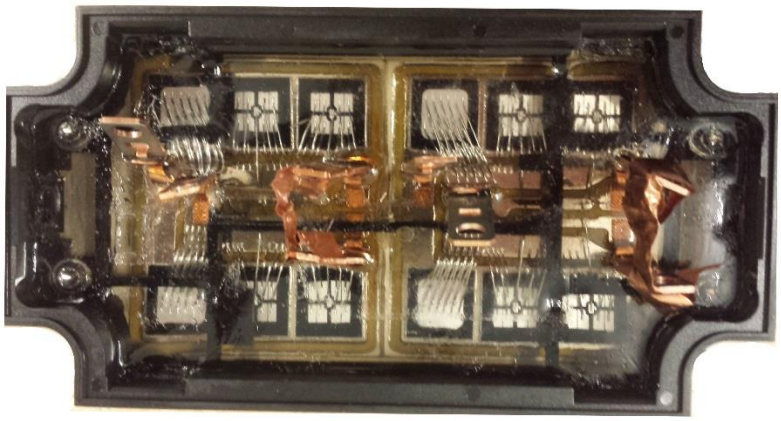

Figure 41 - IGBT #1 after 14 days of MIDEL

8.1.2 Blocking Voltage Test

IGBT Module #	Voltage (Collector-Emitter)	Leakage Current (Upper / Lower)
1	6.5 kV	8.4 µA / 9.1 µA
2	6.5 kV	10.4 µA / 12.7 µA

Module #1 has a small increase and module #2 a small decrease in leakage current after exposure to the liquids. The changes are so small that no clear liquid-effects can be deducted due to measurement inaccuracy. This indicates that exposure to the liquids has not influenced the blocking voltage test on the IGBTs.

8.1.3 Forward Voltage Test

Lower IGBT Module #	Current I_{ce}	Forward voltage drop V_{ce}
1 / 2	10 A	1.529 V / 1.527 V
1 / 2	20 A	1.788 V / 1.784 V
1 / 2	30 A	1.975 V / 1.968 V
1 / 2	40 A	2.128 V / 2.121 V
1 / 2	50 A	2.265 V / 2.256 V
1 / 2	60 A	2.390 V / 2.379 V
1 / 2	70 A	2.507 V / 2.494 V
1 / 2	80 A	2.617 V / 2.604 V
1 / 2	90 A	2.723 V / 2.708 V
1 / 2	100 A	2.825 V / 2.809 V
1 / 2	110 A	2.923 V / 2.907 V
1 / 2	120 A	3.020 V / 3.003 V
1 / 2	125 A	3.068 V / 3.049 V

Changes from before and after the exposure to liquids are below 1 % on both IGBTs. The liquids did not give any major effect on the forward voltage results.

8.1.4 Gate Threshold Test

IGBT Module #	Collector-Emitter current	Applied voltage (Upper / Lower)
1	10.00 mA	5.862 V / 5.884 V
2	10.00 mA	5.899 V / 5.879 V

Changes from before and after the exposure to liquids are below 1 % on both IGBTs. The liquids did not give any major effect on the gate threshold results.

8.2 DC-link Capacitor

The metalized polypropylene capacitor was first exposed to 14 days of MIDEL and cleaned with isopropanol. Afterwards it was exposed to 14 days of Galden and cleaned with isopropanol. During operation and testing, no problems occurred with the capacitor. Measurements were performed after the last cleaning.

8.2.1 RLC-measurement

Test frequency	Capacitance	Θ - angle
50 Hz	4.8862 µF	-90.0 °
1000 Hz	4.8903 µF	-89.9 °

A very small decrease in capacitance is measured (< 1 %), this could be a results of some self-healing occurrences during testing at high voltage.

8.3 Concept Gate Driver

The Concept gate driver was exposed to the same liquid and cleaning procedure as the DC-link capacitor. The only problem experienced with the gate driver was the turn-on delay described in chapter 6.1. Visual inspection after cleaning showed no sign of degradation or damage.

9 Discussion

When constructing the test setup several safety-functions was implemented to ensure a safe operation of the equipment. The most important one is the safety-relay that automatically discharges the capacitor if the test-cabinet is opened. This ensures that direct contact with high voltage is not possible. The complete design of the setup was planned together with Kjell Ljøkelsøy from SINTEF Energy Research, who has a good knowledge in construction of high voltage test-cells. Arne Petter Brede from SINTEF Energy Research, together with Halsten Aastebøl and Bård Almås from NTNU, assisted in performing a risk evaluation and confirming the safety-features of the test-cell. Ole Christian Spro from SINTEF Energy Research aided in the start-up period of the test-cell. Involving 5 people with HSE-experience from other high voltage experiments ensured a safe and operable setup for the high voltage single and double pulse tests.

Several modifications were performed during construction and testing, where the most important ones are mentioned in chapter 6 and the majority of them are related to measurement-equipment and accuracy of measurements. However, the turn-on delay of the gate driver described in chapter 6.1 is an important observation that need consideration when designing for fibre-optical communication in liquids. The results from the fibre-test in MIDEL was only a short-term test for 14 day. It is most likely the reduction off light due to direct damping from the MIDEL that caused the signal-delay. Any long-term degradation of the optical cable or opto-coupler should be further investigated when designing a converter with optical interfaces.

Pre- and post-characterization of the test-components was performed with the same test-equipment and is a good indication on short term effects of insulating liquids on IGBTs protected with gel. The pre- and post-results were very similar and the difference is most likely a result of inaccurate test equipment. A long term study on how the IGBT-modules will react to Galden or MIDEL would give valuable information towards realizing a fully operable pressurized converter-module. Reliability is critical in subsea operations which is why a continuous long term test in liquid should be performed, including a pressurization of the liquid. SINTEF Energy Research is currently working on realizing a converter bridge-leg to be operated in pressurised MIDEL. Rinsing the components with isopropanol was assumed not to effect the components due to the short exposure time.

The results from tests performed in MIDEL in chapter 6 was very similar to the results obtained in air. The temperature was kept as constant as possible. Any variation in temperature could result in noticeable variations of test-results. A 4 % decrease in maximum current at turn-off was observed at the single pulse test. This could be because of the MIDEL, but it is most likely a result of turn-on delay or time-variation from the FPGA-board, since only nanosecond variations could result in this disparity. In the double pulse test, the peak current has a 3% decrease. The results shows that MIDEL is a good insulating liquid alternative since no breakdown or large changes occurred during testing. SINTEF Energy Research has confirmed long-term compatibility issues with MIDEL in direct contact with gel on IGBTs. This could be further investigated in later research using the high voltage test cell constructed in this thesis. Tests were performed in the MIDEL each third day during the 14 day test-period. There were no significant changes and the relative humidity level was kept approximately constant.

The results from tests performed in Galden in chapter 6 was also very similar to the results obtained in air. The temperature was one degree higher in this test then in air, which could create some variations in the measurements. A 6 % decrease in peak current at turn-off was observed at the single pulse test compared to air. It is somewhat lower than the tests performed in MIDEL, which could be a result of a small constant turn-on delay. The increase of light from the optical sender could not be increased further due to datasheet limitation. There was however no breakdown and no larger changes in the Galden tests. The results indicates that Galden is a good insulating liquid alternative for subsea power electronics. SINTEF Energy Research has found that there is a no compatibility issue with Galden and the IGBT gel, rendering it as a more suitable liquid for long-term operations.

The metalized polypropylene capacitor did not experience any large changes from exposure to MIDEL and Galden. It is assumed compatible with both liquids. SINTEF Energy Research have had issues operating this capacitor in pressure. Further testing in liquid and pressure could be performed.

The Concept gate driver was successfully tested in both liquids. The optical connection did create some problems, which was partially resolved by increasing the light from the optical sender. No other major issues arose with the gate driver.

10 Conclusion

The first part of this thesis provided theory regarding the main components needed in a subsea converter. Focus is spent on the IGBT and test-methods for this component, as it is evaluated as one of the most critical components to operate in liquid and pressure. Single and double pulse tests for IGBTs are described.

A safe and fully functional test cell for high voltage single and double pulse tests was constructed and approved for operation, both by NTNU and SINTEF Energy Research. A custom wound air-core inductance was constructed at the NTNU workshop to provide a load for the pulse testing.

The insulating liquids MIDEL 7131 and Galden HT230 are described. Humidity-requirements for the liquids are compared to IEC-standards and chosen at 5 % RH in MIDEL and 25 % RH in Galden. Only a small increase in the humidity was observed during the 14 day test of each liquid proving a sufficient closed environment of the test-setup.

Pre-characterization of components and successful high voltage pulse tests was performed in air as a reference. Two IGBTs was tested for a 14 day period, one in MIDEL and one in Galden. Results from testing and post-characterization showed that both liquids are suitable filling liquids in a pressurized converter for subsea use. MIDEL showed some compatibility issues with swelling of the gel on the IGBT. Galden does not have this issues and is therefore regarded as the preferable filling liquid.

Optical communication in liquids gave a weakening of the fibre optical-link. In realizing a full size converter with optical communication, it is important to account for this loss when dimensioning the strength of the sender and receiver.

11 Further Work

The test cell constructed during this thesis will be of good use for further pulse-testing of other IGBT-modules. Other insulating liquids can also be tested using the same container and setup. The long-term effect of exposing power electronic components to liquids should be tested with regular high voltage pulse tests to ensure an operable and reliable subsea converter in the future.

Tests on IGBTs without gel, or with a protective layer on top of the gel, should be performed since this would eliminate the compatibility-issues with MIDEL and gel. Studies to find critical values in humidity-level or temperature-change could be performed.

Pressurization-tests of a complete phase-leg should be constructed. This would involve a more complicated test-cell, which would have to be approved for pressure. SINTEF Energy Research are currently constructing a test-cell with possibility of continuous inverter-operation under pressure. The test-cell constructed in this thesis would then be a good pre-test of components before they are put in a continuous pressurized high voltage test.

12 References

[1] B. Rasch, "Subsea Electric Power," in *IEEE Norway Section, Power Electronics Chapter*, Bratsbergvegen 5, 2014.

[2] M. Hernes and R. Pittini, "Enabling pressure tolerant power electronic converters for subsea applications," in *2009 13th European Conference on Power Electronics and Applications, EPE '09, September 8, 2009 - September 10, 2009*, Barcelona, Spain, 2009.

[3] K. Holmefjord, "High Power Subsea Solutions," Project Report2014.

[4] R. Pittini and M. Hernes, "Pressure-Tolerant Power Electronics for Deep and Ultradeep Water," *Facilities and Construction Journal,* 2012/2/1/ 2012.

[5] N. Mohan and T. M. Undeland, *Power electronics: converters, applications, and design*: John Wiley & Sons, 2007.

[6] A. Volke and M. Hornkamp, *IGBT modules: technologies, driver and application*: Infineon Technologies AG, 2011.

[7] M. H. Rashid, *Power electronics handbook: devices, circuits and applications*: Academic press, 2010.

[8] M. Hernes, *Power electronic conversion systems for the future subsea power supply: prospects based on experience from two competence building projects on subsea power supply* vol. TR A7161. Trondheim: SINTEF energi, 2011.

[9] R. Pittini, M. Hernes, and A. Petterteig, "Pressure tolerant power electronics for deep and ultra-deep water," in *Offshore Technology Conference*, 2011.

[10] A. Petterteig, R. Pittini, M. Hernes, and O. Holt, "Pressure tolerant power IGBTs for subsea applications," in *Power Electronics and Applications, 2009. EPE'09. 13th European Conference on*, 2009, pp. 1-10.

[11] I. T. AG. Datasheet information on power semiconductors, FZ250R65KE3 [Online].

[12] A. Wintrich, U. Nicolai, W. Tursky, and T. Reimann, "Application manual power semiconductors," 2011.

[13] D. U. Nicolai. (2014, Application Note AN 1403 Determining switching losses of SEMIKRON IGBT modules

[14] J. Lamp, "IGBT Peak Voltage Measurement and Snubber Capacitor Specification," *Application Note AN-7006, SEMIKRON,* 2008.

[15] H. Dicken, "SELF HEALING OF FILM CAPACITORS," Reliability Analysis Laboratory2010.

[16] Spellman. Instruction Manual SL Series [Online].

[17] M. I. Materials. MIDEL 7131 Transformer fluid, Technical Data Sheets [Online].

[18] M. I. Materials. MIDEL 7131 Synthetic Ester Transformer Fluid [Online].

[19] Solvay. Galden® PFPE Testing Electronic Fluids [Online].

[20] Solvay. GALDEN(R) HT HIGH-BOILING Safety Datasheet [Online].

[21] C. Technologie. 2SC0535T Description and Application Manual [Online].

[22] C. Technologie. 2BB0535T Target Description and Application Manual [Online].

[23] A. Techonologies. HFBR-1528Z Transmitter Data Sheet [Online].

13 Appendix A: Software Functions

Function	Comment
"h"	Help for this program
"r"	Read status of double pulse program
"t1"	Length of 1st pulse, ex: t1=400 us
"t2"	Time between 1st and 2nd pulse, ex: t2=200 us
"t3"	Length of 2nd pulse, ex: t3=400 us
"t4"	Time between each double pulse test, ex: t4=2 s
"tc"	Time into the current pulse before current limitation during pulsing is enabled
"td"	Delay-time, Delay time after current limitation has triggered before pulse goes low
"Im"	Setup of current sensor. This number denotes the maximum rating of the device for one turn. Current measurement follows the formula ax+b, where a is a function of Im.
"I_0"	Current offset, b is equal to I_0.
"I1"	Limit value for when the test is interrupted during the first pulse during double pulse testing. Only active outside current delay time, see tc
"I2"	Limit value for when the test is interrupted during the second pulse during double pulse testing or *the* pulse during single pulse testing. Only active outside current delay time
"reset"	Resets the driver interface board if auto reset strap is placed on that board. This function turns the board quickly on and off
"status"	Print the driver interface board status message. This value is of a single hex value. This message is the same as shown on the interface board display

"sta"	Start the program module for switching to begin
"sto"	Stop the program module for switching to end
"si"	Toggle option. Runs the pulse program for one cycle and then stops
"c"	Toggle option. Runs the pulse program until stopped by user or an error
"ps"	Toggle option. Single pulse mode
"pd"	Toggle option. Double pulse mode
"AL or AH"	Set the switching state of channel A during switching during pulse testing. A channel can have one of the following states: '1' – always on, '0' – always off, 'Q' – pulsed, 'NQ' – pulsed inversely, Same for Channel B and C
"IG"	Read the current setup of channels AL, AH, BL, BH, CL, CH
"PI"	Toggle current regulator mode and see printout of PI settings
"RE"	Set the reference current value for the regulator. This value is compared to that of the current sensor before being fed to the regulator.
"KP"	Proportional gain for PI regulator, Option for the regulator. Used for fine tuning
"T1"	Time constant for PI regulator, Option for the regulator. Used for fine tuning
"L1"	Limit of PI regulator, Option for the regulator. Used for fine tuning.
"PW"	Toggle PWM mode
"f"	Set frequency of PWM unit
"am"	Set amplitude of PWM unit
"hy"	Set hysteresis of PWM unit
"dc"	Set the duty cycle of the second bridge leg. This value sets the duty cycle for the high side channel, and the duty cycle for the lower channel is the inverted signal.

14 Appendix B: Interface Card #2